frontiers | Frontiers in Materials

TYPE Review
PUBLISHED 23 March 2023
DOI 10.3389/fmats.2023.1020649

OPEN ACCESS

EDITED BY
Sidney J. L. Ribeiro,
São Paulo State University, Brazil

REVIEWED BY
Wenli Zhang,
Guangdong University of Technology, China
Qian Mao,
The Pennsylvania State University (PSU), United States

*CORRESPONDENCE
Priscilla Brosler,
broslerp@ua.pt

SPECIALTY SECTION
This article was submitted to Carbon-Based Materials, a section of the journal Frontiers in Materials

RECEIVED 16 August 2022
ACCEPTED 14 March 2023
PUBLISHED 23 March 2023

CITATION
Brosler P, Girão AV, Silva RF, Tedim J and Oliveira FJ (2023), In-house vs. commercial boron-doped diamond electrodes for electrochemical degradation of water pollutants: A critical review.
Front. Mater. 10:1020649.
doi: 10.3389/fmats.2023.1020649

In-house vs. commercial boron-doped diamond electrodes for electrochemical degradation of water pollutants: A critical review

Priscilla Brosler*, Ana Violeta Girão, Rui F. Silva, João Tedim and Filipe J. Oliveira

Department of Materials and Ceramic Engineering, CICECO—Aveiro Institute of Materials, University of Aveiro, Aveiro, Portugal

Boron-doped diamond (BDD) electrodes are eco-friendly and widely used in efficient water remediation through electrochemical advanced oxidation processes (EAOPs). These anodes can completely mineralize a wide range of pollutants, only requiring electrical energy. Over the last 2 decades, numerous commercially available BDD electrodes have emerged, but little is known about their electrooxidation performance, particularly if compared to laboratory-produced anodes by different research groups. In this critical review, a comparison between in-house-made and commercially available BDD electrodes based on a systematic literature review (SLR) is carried out. SLR was quite useful in locating and selecting the scientific publications relevant to the topic, enabling information gathering on dissemination, growth, and trends in the application of BDD electrodes in the degradation of water pollutants. More specifically, data concerning the origin of the employed BDD electrodes, and their physicochemical properties were extracted from a thorough selection of articles. Moreover, a detailed analysis of the main parameters affecting the BDD electrodes' performance is provided and includes selection and pre-treatment of the substrate material, chemical vapor deposition (CVD) method, deposition parameters, characterization methods, and operational conditions. This discussion was carried out fully based on the numerous performance indicators found in the literature. Those clearly revealed that there are only a few analogous points across works, demonstrating the challenge of establishing an accurate comparison methodology. In this context, we propose a figure-of-merit equation which aims at normalizing BDD degradation results for a specific contaminant, even if working under different experimental conditions. Two case studies based on the degradation of solutions spiked with phenol and landfill leachate treatment with commercial or in-house-made BDD electrodes are also presented. Although it was not possible to conclude which electrode would be the best choice, we propose a set of guidelines detailing a consistent experimental procedure for comparison purposes in the future.

KEYWORDS

bibliometrics, doped diamond, cvd, electrooxidation, wastewater, commercial electrodes, energy consumption

1 Introduction

Over the last 2 decades, boron-doped diamond (BDD) has gained increased attention and has been extensively studied for electrochemical applications due to its distinct physical and chemical properties from conventional electrode materials. These include a wide electric potential window in aqueous and non-aqueous solutions (Swain et al., 2013; Martin et al., 2019), good stability and corrosion resistance (Ramesham and Rose, 1997; Swain, 2019), inert surface with low adsorption (Swain, 1994), low double-layer capacitance and background current (Swain and Ramesham, 2002), high current density electrolysis (1–10 $A.cm^{-2}$) (Luong et al., 2009), and high overpotential for both hydrogen and oxygen evolution (Martin et al., 2019).

The electric potential window of BDD electrodes is much wider than that of any other material (Brillas and Martínez-Huitle, 2011), with the hydrogen evolution reaction (HER) starting at about −1.2 V/SHE (Standard hydrogen electrode) and the oxygen evolution reaction (OER) at approximately +2.3 V/SHE (Swain et al., 2013; Martin et al., 2019). This broad potential window arises from the BDD's high overvoltage for water splitting (Brillas and Martínez-Huitle, 2011). The HER and OER are inner-sphere reactions that generally consist of multi-step electron transfer reactions that depend on reaction intermediates' adsorption (He et al., 2019). The carbon sp^3-hybridized orbitals in diamond show weak adsorption ability towards these intermediates and, consequently, the catalytic effect for HER and OER in BDD electrodes is weak (Brillas and Martínez-Huitle, 2011). The diamond sp^3-hybridized orbitals form strong covalent bonds and are responsible for the BDD's good stability and corrosion resistance. Studies have shown that BDD electrodes are stable in strong acid media, even for long-term cycling of potential ranging from hydrogen to oxygen evolution reaction overpotentials (Ramesham and Rose, 1997; Swain, 2019). Electrodes based on conventional materials such as glassy carbon or graphite usually have higher surface adsorption ability, forming a polymeric adhesive film on their surface, leading to electrode fouling (Luong et al., 2009). The sp^2-hybridised orbitals present in the surface of these electrodes increase the adsorption strength (Medeiros de Araújo et al., 2014), while the sp^3-hybridised orbitals present in the diamond structure shows weak adsorption capacity (Brillas and Martínez-Huitle, 2011). Electrode fouling is easily avoided in BDD electrodes if working above the potential region of water splitting (Iniesta, 2001). BDD electrodes can also be self-cleaned through the polarization of such polymeric films (Ryl et al., 2016). The surface of BDD electrodes resists deactivation processes, showing stable voltametric responses towards $Fe(CN)_6^{4-/3-}$ even after 2 weeks of continuous potential cycling (Swain, 1994). BDD electrodes are also particularly interesting for electroanalysis and sensing applications since they present low background current and consequent low double-layer capacitance, resulting in lower detection limits for trace analysis when compared to other sensors (Stanković and Kalcher, 2016). The above-mentioned excellent electrochemical behavior of BDD electrodes can vary drastically depending on their physicochemical properties.

More important is the role BDD anodes are currently playing in water remediation through OER and the generated oxygen-based radicals that can completely eliminate a wide range of pollutants, including non-biodegradable compounds (Cornejo et al., 2021). Recent reviews on the electrochemical degradation of contaminants with BDD electrodes can be found in the literature (Cobb et al., 2018; Freitas et al., 2019; Ganiyu and Martínez-Huitle, 2019; He et al., 2019; McBeath et al., 2019; Nidheesh et al., 2019; Trellu et al., 2019; Cornejo et al., 2020; Clematis and Panizza, 2021a; Karim et al., 2021; Bogdanowicz and Ryl, 2022; Crispim et al., 2022; De Luna and Bensalah, 2022; He et al., 2022; Mousset, 2022; Oliveira et al., 2022; Wang et al., 2022). These include studies performed using BDD anodes prepared by chemical vapor deposition (CVD), commercially available and in-house-made, and applied in spiked water and real wastewater treatment systems.

In this critical review, we will evaluate if it is possible to compare the performance of commercial BDD electrodes with those produced in-house towards electrooxidation of water pollutants. We will also discuss how the CVD deposition conditions, the physicochemical properties of the anodes, and the electrooxidation process influence the interpretation of the degradation efficiency results. This assessment will be carefully carried out using bibliometric analysis. Afterwards, an attempt will be made to reach a consensus on possible guidelines and/or degradation performance indicators for future comparison of BDD electrodes from different origins.

2 Electrochemical degradation of contaminants with BDD electrodes: A bibliometric analysis

Bibliometrics is a research method that uses quantitative and statistical analysis to describe patterns in publications. Bibliometric studies are frequently used to investigate structural interrelationships and to increase the understanding of a specific subject state of the art (Donthu et al., 2021). In order to properly carry out these studies, it is essential to know Lotka's inverse square laws regarding the calculation of authors' productivity, Bradford's law for the dispersion of authors in different journals, and Zipf's law concerning the frequency of words in each document (Guedes and Borschiver, 2005; Araújo, 2006). Systematic literature review (SLR) was chosen as the method of searching for publications since it is widely used and because it is a structured way of locating and selecting the relevant publications, increasing the reproducibility and reliability of the method (Donthu et al., 2021).

In this work, bibliometric analysis was used 1) to identify the growth and trends in the application of BDD in the degradation of contaminants; 2) to identify the dissemination of information with quantification of publications by journals, universities, and research centers, and by country; and 3) to verify the keywords relationship between themes through their co-occurrence in a network graph. The tools used to visualize the results and create the graphics were Microsoft Excel and VOSViewer (van Eck and Waltman, 2010).

The bibliometric search of the topic "electrochemical degradation of contaminants with BDD electrodes" was carried out by a Boolean advanced search query in the Scopus database through a search string connecting the topics by the title field of publications in April 2022. The details of this search query can be found in the Supplementary Table S1. A total of 875 articles meeting the established criteria were obtained. The search was restricted to

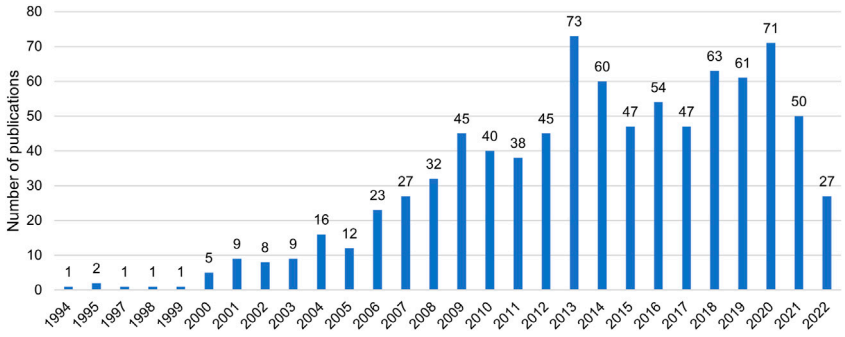

FIGURE 1
Number of publications per year on BDD as an electrode for electrooxidation of contaminants, based on the Scopus database (source: the authors).

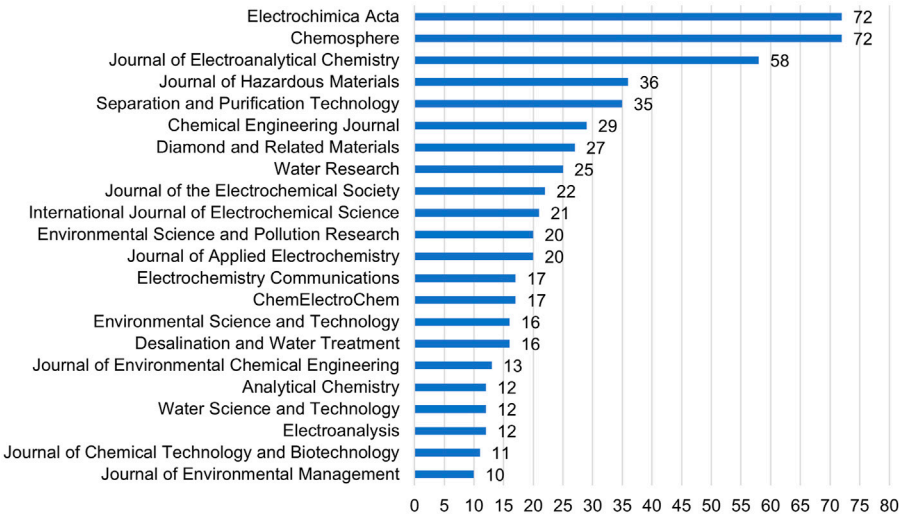

FIGURE 2
Number of publications per journal with more than 10 publications on BDD as an electrode for electrooxidation of contaminants, based on the Scopus database (source: the authors).

scientific articles as the document type and only to the English language. This result went through a process of elimination of duplicates and irrelevant results (not related to the subject), reaching a final number of 868 publications for further bibliometric analysis. The list of strings used in the search query was defined based on a previous broader search in which the fundamental terms used to describe the electrochemical degradation of contaminants were identified (Supplementary Table S2). Figure 1 illustrates the number of publications per year on BDD as an electrode for electrooxidation of contaminants.

The first publication identified in the SLR was published in 1994 (Mitra et al., 1994), although the first one ever reported on the electrochemical behavior of CVD diamond dates back to 1987 (Pelskov et al., 1987). However, the latter does not address pollutant degradation studies. In the early 1990s, studies of BDD used as electrodes began to emerge all over the world: Japan (Patel et al., 1992), the United States (Swain, 1994; Swain and Ramesham, 2002) or China (Zhu J. Z. et al., 1995; Zhu P. et al., 1995). The number of publications increased rapidly in the 2000s, reaching a peak of 73 publications in one single year (2013). Nearly the same number of publications was achieved again in 2020. By the time these data were gathered, early 2022 already accounted for 27 publications, clearly indicating that the topic has excellent scientific relevance and is still extensively explored. The dissemination of information was identified through the analysis of publications by journals, as shown in Figure 2.

Articles on the topic were published in more than 160 different journals. *Chemosphere*, *Electrochimica Acta,* and *Journal of Electroanalytical Chemistry* published around 23% of all the articles on BDD as an electrode for electrooxidation of contaminants. Therefore, researchers on this subject should consult information primarily in these three journals. Figure 3 presents the bibliometric study finding the dissemination of information by universities and research centers with more than 20 publications on the topic, as well as the number of publications per country.

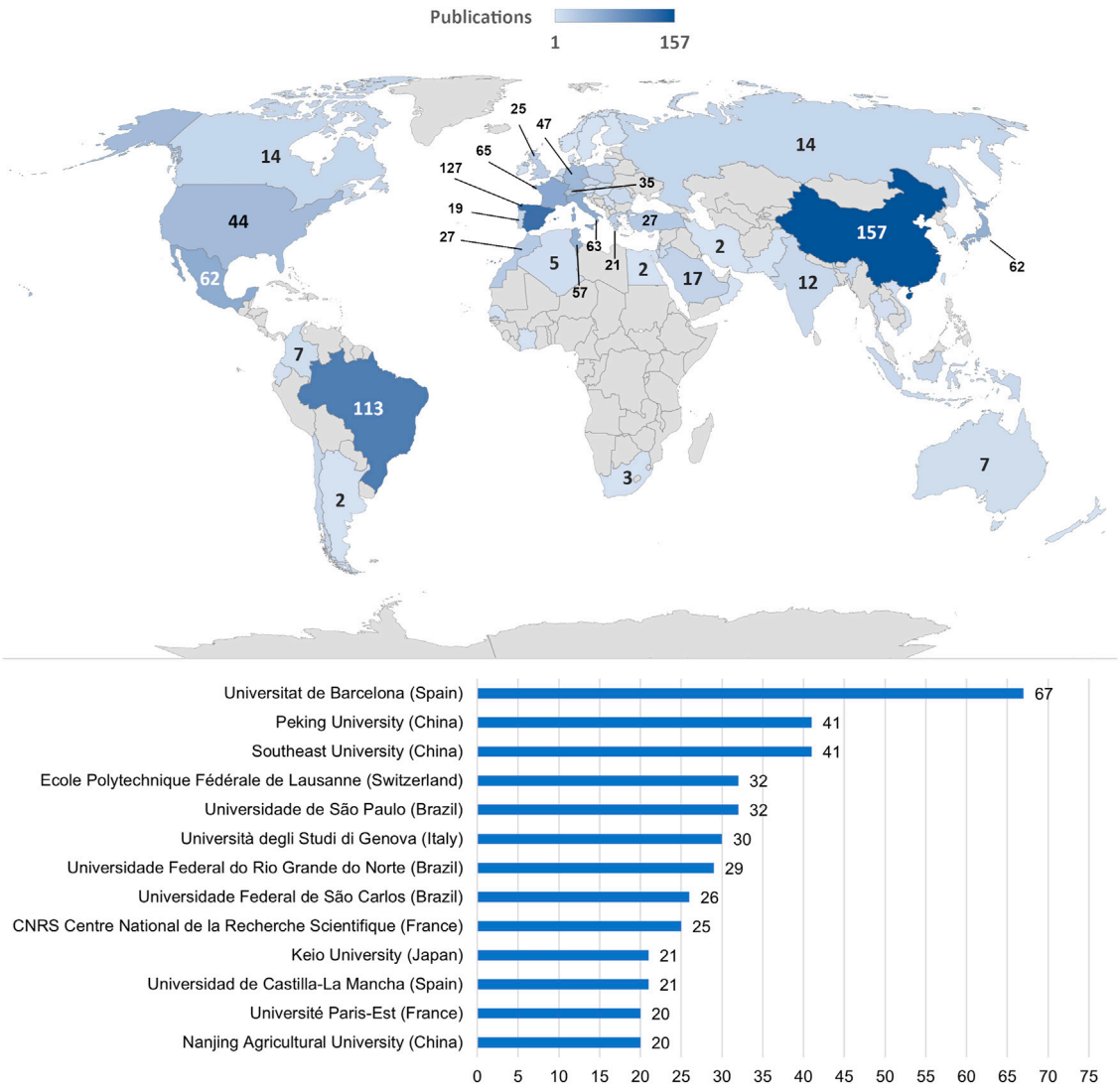

FIGURE 3
Number of publications per university and research center with more than 20 publications on BDD as an electrode for electrooxidation of contaminants (upper); and number of publications per country on BDD as an electrode for electrooxidation of contaminants (below). All results were based on the Scopus database (source: the authors).

The institution contributing the most to disseminating this topic is the Universitat de Barcelona (Spain). Switzerland ranks 11th, but one should note that the École Polytechnique Fédérale de Lausanne has the fourth-highest number of publications on the subject. China, Spain, Brazil, France, Italy, Mexico, and Japan represent more than 50% of publications. The most significant contributors are China with 157 publications, Spain with 127, and Brazil with 113. To identify the trends in the application of BDD anodes in the degradation of contaminants and verify the relationship within the main themes, a keyword network graph (Figure 4) was constructed.

The network graph shows six main clusters where the red highlights response surface methodology studies that encompass cyclic voltammetry measurements to evaluate the electrochemical properties of BDD anodes and the electrooxidation of pollutants. The larger the frame of a given keyword, the more frequent it is across the literature. In the red cluster, pesticides appear as the primarily studied pollutant. The purple cluster represents the analysis of energy consumption by the electrooxidation processes using BDD anodes, and the cyan cluster is mainly related to wastewater disinfection. BDD electrochemistry, electrochemical oxidation of phenol and dyes, and the toxicity of the resulting by-products are featured in the green cluster. The blue one involves water treatment containing pharmaceuticals (primarily studied contaminants) by different EAOPs (anodic oxidation, electro-Fenton, and photoelectron-Fenton). This cluster includes intermediate oxidation products such as carboxylic acids (oxalic, acetic, or formic), often used as models to investigate the reaction mechanisms and electrocatalytic properties of the anode materials (de Queiroz et al., 2017). The yellow group gathers information on the production of hydroxyl radicals and carboxylic acid intermediates during the final

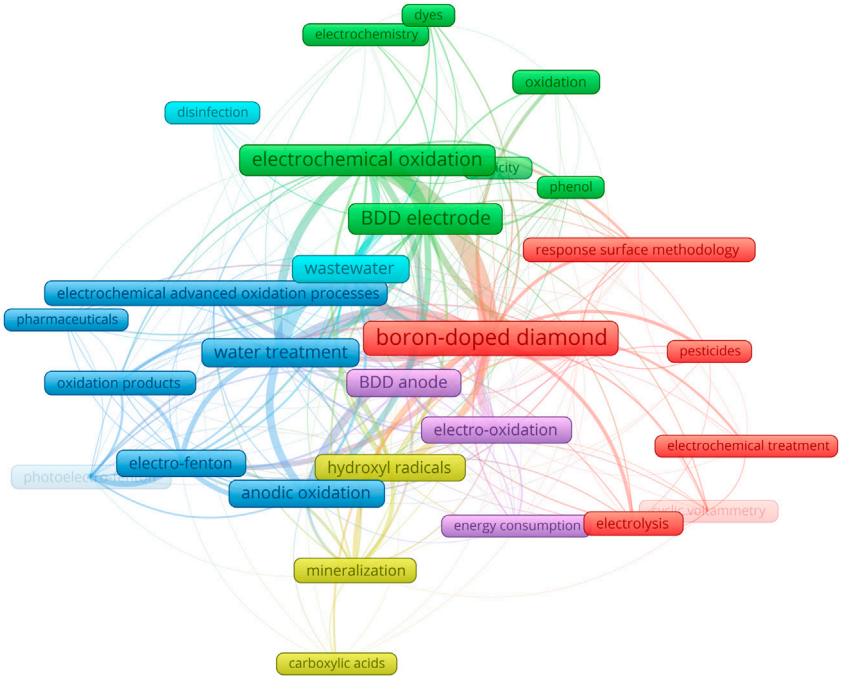

FIGURE 4
Keywords co-occurrence network (minimum of 10 occurrences) representation of the trends on the application of BDD anodes in the degradation of contaminants and corresponding relationship within the main themes, sorted in six clusters represented in different colors, based on the Scopus database and VOSviewer as the bibliometric network graph software (source: the authors).

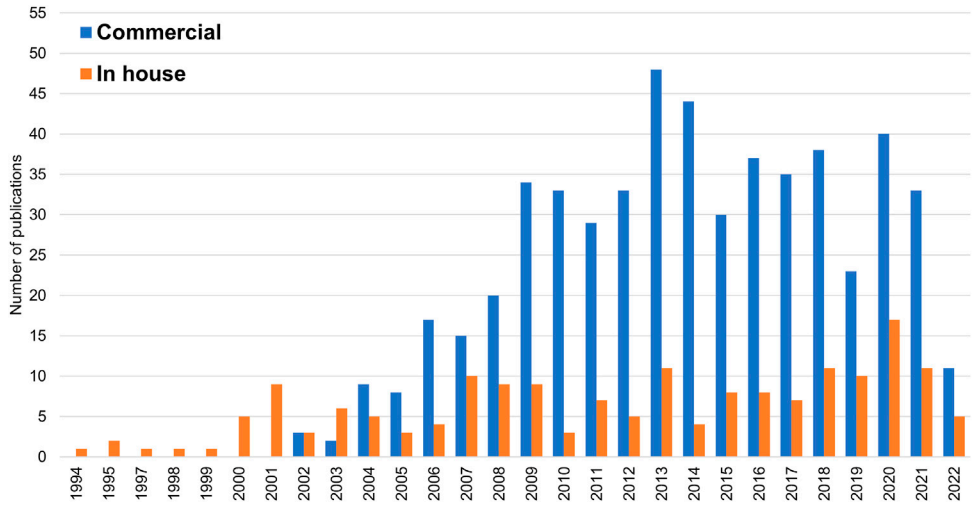

FIGURE 5
Number of publications per year on commercial and in-house BDD anodes in the degradation of contaminants, based on the bibliometric analysis search (source: the authors).

mineralization process. Overall, the keyword network graph in Figure 4 reveals that BDD anodes for water remediation have been primarily used in the electrooxidation of pharmaceuticals, pesticides, carboxylic acids, phenolic compounds, dyes, and for water disinfection of bacteria and viruses.

SLR verified that the degradation of water pollutants through BDD electrodes is a subject particularly targeted in the last 2 decades, highly relevant (mentioned in more than 160 journals) and studied on all continents. The keywords co-occurrence network map allowed the identification of the most studied types of water

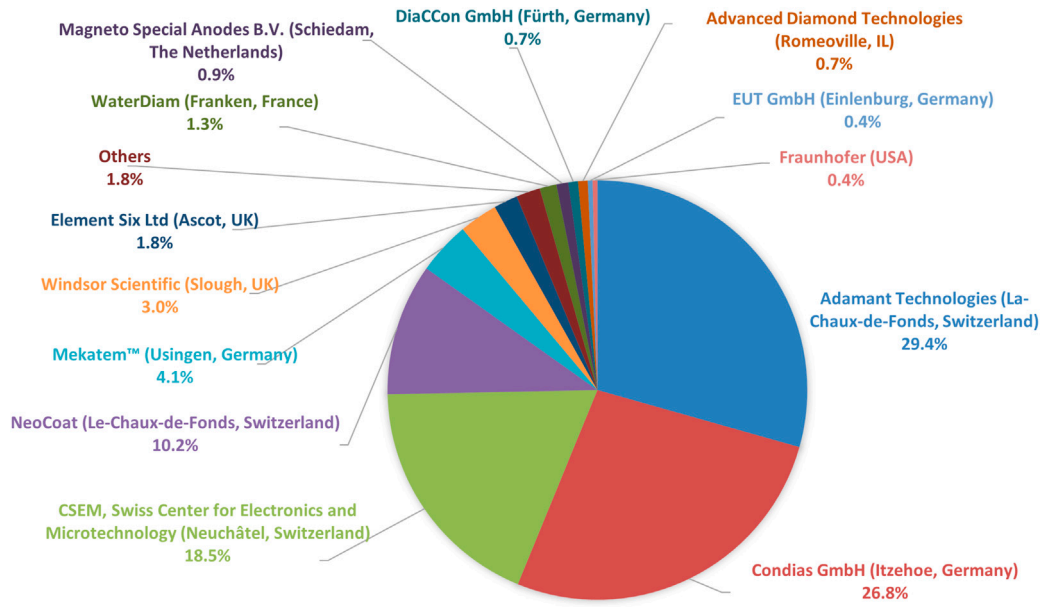

FIGURE 6
Commercial BDD manufacturer preference based on the bibliometric analysis search (source: the authors).

pollutants and applied EAOPs, as well as other relevant issues to the degradation process: the generation of by-products and their toxicity and associated energy consumption/costs.

3 Utilization of laboratory produced and commercial BDD electrodes

From 1994 to 2001, electrooxidation of pollutants using BDD anodes was exclusively performed with lab-made electrodes (Figure 5). Commercial BDD electrodes started to gain ground and were first reported in 2002. The number of studies considering the application of commercial BDD anodes increased, and since 2006 they are around 4 times greater (average) than those using in-house-made electrodes. However, only 20% of the 868 identified publications were related to laboratory-made BDD anodes, and 63% applied commercially available electrodes. The remaining unspecified 17% of the reported studies can probably be associated with commercial BDD electrodes, which would sum up to 80% of the publications implementing such electrodes. Such a high percentage of the use of commercial electrodes may indicate the technology's maturity is being achieved.

Figure 6 shows the distribution of the companies whose BDD electrodes were used in the analyzed publications. A list of commercial BDD suppliers, including companies that did not appear in the articles from the SLR, is available in the Supplementary Table S3. Commercial electrodes from Adamant Technologies (Switzerland) and NeoCoat (Switzerland), which are spin-off companies of CSEM (Switzerland), together with those manufactured by CSEM itself, sum up to 58% of presence in the articles from the SLR, followed by 26.8% from Condias GmbH (Germany), and 4.1% from Mekatem™ (Germany).

Commercially manufactured BDD electrodes may offer greater reproducibility since companies are committed to delivering high quality and reproducible materials to their clients but are also costly and with a fixed set of morphological and electrochemical characteristics, such as sp^3/sp^2 ratio, boron doping level, film morphology and thickness, electrochemical potential window, capacitance, among others. Nevertheless, they enable numerous research groups without in-house CVD equipment to explore the use of such BDD electrodes in their studies, further expanding their application range and effectively contributing to knowledge expansion of these thin films.

The main advantage of producing in-house BDD electrodes is growing customizable films by exploring and controlling their properties, such as the sp^3/sp^2 ratio, thickness, boron doping level, growth rate, and grain size. These properties strongly define the working potential window of the electrode, its conductivity and selectivity. Hence, in theory, precise BDD films can be created and adapted to each type of target pollutant. In addition, in-house BDD deposition allows the exploration of different deposition conditions and/or substrate materials. The full potential of BDD electrodes can only be attained by appropriate and specific electrode design for each application and/or target contaminant (Bogdanowicz and Ryl, 2022).

Non-etheless, in-house BDD film deposition may also imply lower reproducibility, depending on the CVD reactors used and their operability. Additionally, the overall area of the BDD films is limited by the volume and operation design of the CVD chamber reactor (Mehedi et al., 2014), typically smaller than the commercial ones. The in-house production of BDD electrodes is expensive for universities and research centers, when including the cost of the CVD equipment and the process associated costs such as electricity consumption, water cooling system, and reactive gases (Railkar et al., 2000). Furthermore, a well-prepared infrastructure is mandatory to

meet all the necessary safety requirements, including electrical hazards and the use of dangerous reactive gases. These, and the lack of know-how, contribute to limiting the spread of such equipment in laboratories working mostly on water purification processes.

4 BDD electrodes from different sources

It is a challenge to compare the performance of different in-house BDD electrodes regarding the electrooxidation of water pollutants. First, the design and working conditions of the adopted CVD technique can vary widely: the deposition method (hot-filament -HFCVD, or microwave plasma -MPCVD); the experimental deposition parameters (CH_4/H_2 ratio, pressure, substrate temperature, boron doping source, [B]/[C] ratio); and the substrate material and its prior preparation (Gracio et al., 2010; May et al., 2011). Altogether, these parameters will influence the final physicochemical properties of the BDD electrode, such as sp^3/sp^2 ratio, effective boron doping level, grain size, film thickness, electrical conductivity, electrochemical potential window, oxygen evolution potential (OEP), electron transfer rate, surface roughness, and surface termination (May et al., 2011; Salgueiredo et al., 2011; Huang et al., 2021; Sharma et al., 2022).

Second, the application of the BDD anodes in the electrooxidation of contaminants includes several other accountable factors such as the degradation conditions used in the experiments (current density, type of EAOP, pH and type of electrolyte, active electrode area, volume of solution, type and concentration of the pollutant, electrochemical cell design, or fluid dynamics), and the water system itself (spiked water or real wastewater) (Sires et al., 2014; Cano et al., 2016; Xu, 2016; Ma et al., 2018).

The number of publications concerning BDD anodes in electrochemistry has drastically increased due to the emergence of commercial BDD manufacturers. It broadened the application of BDD electrodes resulting in high-quality publications but further entangled possible comparisons between electrodes' performance. Most reports on tested commercial BDD electrodes lack information on their physicochemical properties and preparation process. The manufacturing process of such complex thin films dictates their performance (Einaga et al., 2014), and it may vary significantly from one company to another. In this section, we discuss how these factors control the final physicochemical properties of BDD coatings, hence their implementation in degrading pollutants present in water systems.

4.1 Substrate material and preparation

In the preparation of BDD electrodes, the primary function of the substrate for electrochemical applications is to allow the flow of electric current through the electrode, providing physical support to the thin film and conferring enough mechanical stability to the electrode (Chen, 2004). The first thing to keep in mind is that the substrate nature might influence the BDD final properties. Thus, its selection must meet criteria such as stability under extreme conditions (high current density, intense erosive and/or abrasive wear, and strong acids or bases media) (Yang et al., 2022).

Ideally, the substrate material must withstand the CVD deposition conditions, present high affinity towards diamond thin film growth, high mechanical strength, good electrical conductivity, and electrochemical inertness or the ability to easily form a protective passivation layer on its surface (Chen, 2004; He et al., 2019). A carbide buffer layer may be formed during CVD deposition, restricting further substrate carburization and promoting easy diamond nucleation and crystal growth (Xiang-Liu et al., 1991). Furthermore, a substrate material with low carbon solubility and diffusion coefficient yields higher diamond nucleation rates (Yang et al., 2022). Temperature gradients interfere with the surface reactions and diamond growth kinetics (Bushuev et al., 2017). Therefore, the diffusion coefficient of the carbon atoms, the substrate thermal conductivity, and its coefficient of thermal expansion (CTE) influence the adhesion strength of the diamond thin film, grain size, growth rate, and residual stress, dictating its service life (Yang et al., 2022).

Several materials have been proved suitable substrates for BDD deposition, including Si, Nb, Ta, W, Mo, Ti, Zr, and graphite (Fryda et al., 1999; Shaw et al., 2002; Chaplin et al., 2011); dielectric ceramics (Neto et al., 2012); high pressure-high temperature (HPHT) diamond (Denisenko et al., 2008); carbon fibers (Jian et al., 2021); SiO_2 fibers (Zhang et al., 2020); carbon nanotubes (Zanin et al., 2014); TiO_2 nanotubes (Vernasqui et al., 2021); or metal foams (Zhang J. et al., 2019). Polished silicon wafers are by far the most applied substrate material, being identified in more than 36% of the published articles (Supplementary Figure S1), especially *p*-doped Si commercial wafers. Their characteristic low electrochemical activity and ability to form stable and compact oxide films help prevent film delamination (Brito et al., 2018). However, Si substrates still have many limitations for large-scale applications since they are not suitable in aggressive water treatment environments, mainly due to their relatively low conductivity and brittleness (Yu et al., 2014). Contrary to Si substrates' short durability, Nb/BDD electrodes have shown a lifetime of more than 850 h during electrolysis (0.5 M H_2SO_4) at very high current densities such as 10 A/cm^2 (Fryda et al., 1999). The SLR indicates that currently, the second most used substrate material is Nb, followed by Ti and Ta, which are metals capable of forming stable and protective passivation layers. It is important to emphasize that Nb became the preferred choice of substrate material over the years (Supplementary Figure S2) and, since 2013, started to surpass the use of Si substrates. Roughly, the approximate substrate stability for diamond film deposition obeys the following order: Ta > Si > Nb > W > Ti (Chaplin et al., 2011). The CTE of the substrate material is the main factor influencing its compatibility with the BDD film deposition and ideally, it should be as close as possible to that of diamond ($0.7–2.0 \times 10^{-6}$ K^{-1}) (Moelle et al., 1997; Luong et al., 2009; Gracio et al., 2010). A CTE mismatch can cause delamination of the BDD film with possible consequent corrosion of the substrate due to electrolyte permeation through the thin film (Chaplin et al., 2011). Nevertheless, the high cost of Nb, Ta, and W substrates makes them unattainable for widespread use in large-scale applications (Nidheesh et al., 2019). Ti has been considered a desirable substrate among those mentioned above due to its lower cost, high conductivity, corrosion resistance, and

excellent mechanical properties (Braga et al., 2009). Yet, Ti/BDD electrodes have shown short service life due to the formation of a TiC intermediate layer generated by the diffusion of carbon species onto the metal during the deposition, resulting in a rough and porous structure that promotes early deterioration of the BDD film adhesion and stability (Fryda et al., 1999; Lim et al., 2008; He et al., 2019). The most likely reasons of electrode failure are assumed to be the TiC layer corrosion at the substrate/film interface, the quality and adhesion of the BDD film, the residual stress produced in the CVD process, and the degradation of the diamond film (Lu X. R. et al., 2019). According to Lu et al., the delamination process occurs in two main stages. The first stage of electrode failure is caused mainly by pore-type defects in the BDD films that allow the electrolyte to penetrate the BDD film and corrode the TiC intermediate layer, which is unstable and quickly decomposes causing the BDD film to delaminate from the substrate. The second stage is caused primarily by corrosion holes created in the Ti substrate. Several attempts have been made to improve the service life of Ti/BDD electrodes, such as developing multilayered structures or increasing the boron concentration in the CVD deposition to inhibit the TiC layer growth, with different levels of success (Guo and Chen, 2007; Gerger and Haubner, 2008; Sun et al., 2012; Kwon et al., 2019).

Following the choice of the appropriate substrate material, its pre-treatment for CVD deposition may also affect the final characteristics of the BDD film. The surface properties of the substrate influence the diamond film roughness, adhesion strength, and electroactivity (Guimaraes et al., 2020). Diamond growth over non-diamond materials usually requires pre-treatment of their surface by a seeding stage (Spitsyn et al., 1981). This is necessary to obtain proper diamond nucleation density with a complete and packed growth of the thin film, without any substrate area exposed to the solution, which could compromise the working electrode. An effective seeding process depends on the size of the diamond abrasive particles, processing time, and the adopted method (e.g., manually scratching, ultrasonic bath). There are a few studies reporting on the effect of substrate preparation on the nucleation and growth of BDD films (Chaplin et al., 2011; da Silva et al., 2018) showing that ultrasonic seeding is more effective than seeding through manual scratching. In addition, a rougher Nb substrate prepared by sandblasting with alumina particles (75–106 μm) resulted in the most effective electrode lifetime compared to that with the untreated substrate or the sandblasted one with smaller alumina particles (Choi et al., 2017).

Considering the direct influence of the substrate material on the electrochemical properties of BDD, when Nb/BDD (planar) and Ti/BDD (Ti mesh) electrodes were compared for phenol degradation, Nb/BDD showed the best performance (Hangarter et al., 2015). However, the electrodes had different geometries (consequently, different specific areas), boron doping levels, and different film thicknesses, limiting comparisons between the different metallic substrates. Si/BDD and Nb/BDD electrodes have been compared in different studies for the electrooxidation of acid violet 7 dye (Brito et al., 2018) and norfloxacin (da Silva et al., 2018). In both cases, the Si/BDD electrode showed higher removal rates with lower associated energy consumption. BDD films deposited over Nb, Si, Ti, and TiNx/Ti by HFCVD were compared in terms of their performance, particularly chemical oxygen demand (COD) removal and *Escherichia coli* sterilization from livestock wastewaters (Kwon et al., 2019). The TiNx/Ti/BDD electrode with a TiNx intermediate layer showed better performance and higher service life than Nb/BDD, Si/BDD, and Ti/BDD. It is quite difficult to evaluate the effect of the substrate material on the BDD electrodes' performance since the published experimental conditions and parameters are not described in detail. Finally, a recent study (Yang et al., 2022) is perhaps the most systematic and complete comparison to determine the substrate effect, providing enough detailed information on the BDD deposition and substrate preparation conditions and characterization. The influence of the substrate material (Si, Ta, Nb, and Ti substrates) was examined in terms of electrochemical properties, microstructure, degradation of the antibiotic tetracycline, and service life of the identically deposited BDD films. Their results showed that the physicochemical properties of the substrate have a significant impact on the growth and microstructure of the BDD film, and the growth rate followed: Si > Ta > Nb ≫ Ti. In addition, the surface finish of both substrate and BDD film also influenced the performance of the BDD electrode. The Ti/BDD electrode showed the best performance in terms of OEP, background current, electron transfer kinetics, and energy consumption, but far shorter service life than Si/BDD, Ta/BDD, and Nb/BDD. In terms of tetracycline removal and current efficiency, the performance of the electrodes followed: Si/BDD > Ti/BDD > Nb/BDD > Ta/BDD. Yang et al. indicated that the type of substrate does not significantly affect the boron doping level and diamond quality of BDD electrodes. However, they suggest that the degradation performance of BDD electrodes is affected by the intermediate carbide interlayers formed in the interface between the substrate and the BDD film during CVD deposition. These interlayers are closely related to the substrate material and affect film thickness, grain size, and electron transfer resistance, thus the surface state of BDD films and, consequently, their organics electrooxidation capability.

Laboratory and pilot tests on wastewaters have been successful in showing the feasibility of BDD electrodes (Li et al., 2014; Bergmann et al., 2015; Wu et al., 2015; Alvarez Pugliese et al., 2016; Souza et al., 2016; Naji et al., 2017; Durán et al., 2018; Salmerón et al., 2019; Roccamante et al., 2020; Tawabini et al., 2020; Maldonado et al., 2021; Monteil et al., 2021; Salmeron et al., 2021), but the absence of a universally appropriate and accepted substrate with a defined size and established durability are a tremendous challenge for large scale application of such anodes. Furthermore, practical long-term application of BDD electrodes (highly stable under anodic polarization) in the degradation of pollutants is still subjected to failure at high applied current densities (e.g., 1 $A.cm^{-2}$), mainly due to poor film adhesion with consequent film delamination (Chaplin, 2014).

The above literature analysis demonstrates that evaluation of the substrate effect on the BDD electrode final performance is not straightforward. It depends on numerous factors leading to very different conclusions. Hence, a further detailed and systematic research is required, and it should also include the complete analysis of the microstructure and physicochemical properties of BDD films like grain size, surface roughness, growth rate, conductivity, sp^3/sp^2 ratio, residual stress, adhesion strength, electron transfer rate, OEP, electrochemical potential window,

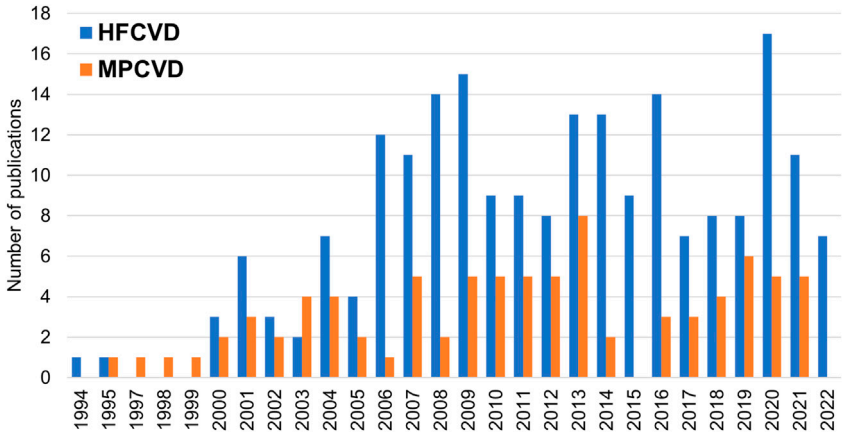

FIGURE 7
Number of publications per year on commercial and in-house BDD anodes, employing HF or MPCVD deposition methods, based on the bibliometric analysis search (source: the authors).

background current, and boron doping level, deposited under the same CVD deposition conditions over several different substrate materials. Then, possible guidelines may be provided for adequate selection of substrate material for the deposition of BDD thin films for specific water treatment applications.

4.2 The chemical vapor deposition process

CVD diamond thin films are usually carried out by activating a mixture of a carbon-containing gas (usually methane in low concentration) with molecular hydrogen. During its course, carbon radicals are generated and react with dissociated hydrogen in high concentration to give the diamond growth precursors (Yang et al., 2019). Chemical vapor deposition techniques include hot-filament (HFCVD), RF-plasma (RFCVD), microwave plasma (MPCVD), and related DC plasma, DC arc-jet, or oxy-acetylene flame (Srikanth and Jiang, 2011). Regarding BDD film deposition, SLR detailed analysis indicates that 71.2% of the articles employed hot-filament (HFCVD) and 28.8% microwave plasma (MPCVD), as illustrated in Figure 7.

In HFCVD deposition, an appropriate filament temperature will guarantee molecular hydrogen dissociation, usually obtained at temperatures above 2000°C. The melting point and purity of the metallic filaments (e.g., W, Ta, and Re) are always considered to avoid or minimize their degradation, which causes film contamination (Mehta Menon et al., 1999). Suitable diamond growth kinetics is also dependent on the distance between each of the filaments and that between them and the substrate's surface. In MPCVD, the microwave power and frequency are the important parameters that require careful control and optimization. Microwave frequency can vary from 300 MHz to 300 GHz, with most depositions performed in commercial reactors (e.g., Seki-ASTeX reactors) typically at 2.45 GHz (Schwander and Partes, 2011). MPCVD depositions using higher microwave powers exhibit increased feed gas temperature and dissociation efficiency, resulting in larger grain sizes and improved growth rates (Tang et al., 2011).

Manufacturers of commercial diamond films tend to adopt the HFCVD method due to the possibility of growing films over large surface areas, similarly to some authors who implemented such method to deposit BDD films over areas as large as 0.5 m^2 (Haenni et al., 2004). In contrast, MPCVD enables higher growth rates, higher phase purity, and better reproducibility since HFCVD temperatures are limited to the filaments' melting point, restricting the concentration of dissociated hydrogen atoms (Macpherson, 2015). The latter is the main reason for using MPCVD in free-standing diamond deposition (Schwander and Partes, 2011). In addition, the degradation of the filaments used in HFCVD can promote metal contamination of the films (Schwander and Partes, 2011), interfering with the quality of the final films and, for example, hindering the film adhesion to the substrate or inducing graphitization points (Griesser et al., 1994; Mehta Menon et al., 1999; Lee et al., 2022). On the other hand, the plasma area is limited by the wavelength of the microwave radiation in the MPCVD method (Macpherson, 2015), greatly restricting industrial-scale production of BDD electrodes for pollutant degradation. The preference for HFCVD is also explained by the simplicity of its apparatus and lower cost compared to MPCVD (Gracio et al., 2010).

As demonstrated in the previous section, a comparison between the distinct deposition parameters used in the production of commercial and in-house electrodes constitutes a challenge. Each CVD reactor has specific dimensions and characteristics, as well as optimized deposition parameters (Einaga et al., 2014). For example, two different reactors using the same deposition conditions will not necessarily yield similar BDD films with the very same characteristics due to geometric constraints within the reactor that directly affect the deposition kinetics (Parikh and Adomaitis, 2006). Tables 1, 2 summarize some of the HFCVD and MPCVD deposition parameters respectively, found in the articles within the SLR.

TABLE 1 HFCVD deposition conditions present in the literature based on the bibliometric analysis search.

University, research center, or commercial manufacturer	Substrate	CH_4/H_2 (%)	Boron source	Filament temperature (°C)	Substrate temperature (°C)	Pressure (mbar)	[B]/[C] (ppm)	Ref.
Adamant Technologies (Switzerland)	p-Si; Ti	1.0%	Trimethylborane	2,440–2,560	830	—	100–8,000	Pujol et al. (2020)
Condias GmbH (Germany)	Nb	0.5%–2.5%	Diborane	2,200–2,600	700–925	10–50	500–8,000	Chen et al. (2014)
CSEM, Swiss Center for Electronics and Microtechnology (Switzerland)	p-Si	1.0%	Trimethylborane	2,440–2,560	830	—	800–8,000	Machini et al. (2016)
Central South University, China	Si; Ta; Nb; Ti	1%–4%	Diborane	2,200–2,400	650–850	30	2000–20,000	Zhu et al. (2018), Miao et al. (2022)
	Si	3.0%	Diborane	—	850	20	—	Li et al. (2020)
École Polytechnique Fédérale de Lausanne (EPFL), Switzerland	p-Si	1.0%	Trimethylborane	2,440–2,560	830	—	2,500–10,000	Kapałka et al. (2009)
	—	1.0%	Trimethylborane	—	760–870	10–100	600	Lévy-Clément et al. (2003)
Instituto Nacional de Pesquisas Espaciais (INPE), Brazil	Ti	0.5%–5.0%	B_2O_3	—	650	53–67	100–30,000	Migliorini et al. (2016)
Jilin University, China	Ti	1.0%	Trimethylborate	2,000	—	70	8,000	He et al. (2016)
Slovak University of Technology in Bratislava, Slovak Republic	n-Si	1.0%	Trimethylborane	—	650 ± 20	30	10,000	Kuchtová et al. (2020)
	Si	2.0%	Trimethylborane	2,100	650	30	10,000	Mackuľak et al. (2020)
Tianjin University of Technology, China	Ta	2.0%	Trimethylborate	—	950	50	—	Li et al. (2018)
	Ta	0.7%	B_2O_3	—	800–1,000	~67	—	Jiang et al. (2008)
	Ta	0.7%	B_2O_3	2,000	800	25	—	Chang et al. (2009)
Zhejiang University, China	Ta	2.0%	Diborane	2,500	800	50	—	Li et al. (2015)

*TMD, trimethylborane

CVD polycrystalline diamond deposition is generally performed using a CH_4/H_2 gas mixture, with microcrystalline (MCD) and nanocrystalline diamond (NCD) being typically grown under hydrogen-rich gas mixtures. The introduction of argon into the gas mixture increases the diamond re-nucleation rate, preventing enlargement of the crystallites, and ultra-nanocrystalline diamond (UNCD) is usually grown under argon-rich CVD environments (Gracio et al., 2010). According to the van der Drift regime (van der Drift, 1967; Gracio et al., 2010), MCD and NCD grain size and thickness are determined by the deposition time, while UNCD presents a nodular morphology with negligible crystal faceting, disobeying the standard regime (van der Drift, 1967; Yang et al., 2019). Some researchers also add small amounts (<2%) of O_2 to the gas mixture to limit impurity incorporation and non-epitaxial defect formation (Teraji et al., 2015). The gas mixture influences the grain size, diamond quality, and the surface finish of the diamond film (Neto et al., 2016). The temperature of the substrate plays a significant role in the film growth kinetics. MPCVD diamond growth was evaluated over HPHT diamond substrates in a broad range of substrate temperatures (750°C–1,150°C) and CH_4/H_2 gas mixture ratios (1%–13%) (Bushuev et al., 2017). Results showed that an appropriate substrate temperature could significantly improve growth rate, and higher CH_4/H_2 ratios favor enhanced growth rates. Increasing CH_4 content leads to enhanced non-diamond carbon incorporation. Competitive etching by atomic hydrogen showed a strong effect at low CH_4/H_2 ratios (1%), and a transition from growth to etching was observed at substrate temperatures higher than 1,000°C and low CH_4 concentrations (1%–4%).

Application of a direct bias current between the filaments and the substrate is not mandatory, but doing so can enhance nucleation

TABLE 2 MPCVD deposition conditions present in the literature based on the bibliometric analysis search.

University, research center, or commercial manufacturer	Substrate	CH_4/H_2 (%)	Boron source	Substrate temperature (°C)	Pressure (mbar)	Power (kW)	[B]/[C] (ppm)	Ref.
Keio University, Japan	p-Si	—	Trimethylborate	—	—	5	2000–10000	Triana et al. (2020)
	Si	—	Trimethylborane	—	~113	5	—	Yamaguchi et al. (2019)
Michigan State University, United States	p-Si	0.5%–1%	B_2O_3	850	~47	1.0–1.3	100–1,000	Witek and Swain (2001)
Peking University, China	Ti	1%–2%	Diborane	800	~53	1.2	1,000–5,000	Wei et al. (2011)
University of Technology, Poland	p-Si	1.0%	Diborane	1,000	~67	1.3	1,000–10000	Ryl et al. (2019)
University of Tokyo, Japan	n-Si	0.5%	B_2O_3	800–900	~153	1.5	8,000	Lévy-Clément et al. (2003)
	p-Si	3.0%	Diborane	880	40	—	6,000	Lévy-Clément et al. (2003)
	n-Si; p-Si	3% ± 1%	B_2O_3	800–900	~153	5	10000	Mitadera et al. (2004), Kondo et al. (2007)
Utsunomiya University, Japan	p-Si	—	B_2O_3	540	~93	1.4	10000	Murugananthan et al. (2011)

*TMD, trimethylborane.

density during the deposition and improve diamond quality (Sein et al., 2006). The gas pressure may change the mean free path of particles (primarily hydrocarbons radicals) and, in consequence, their activity due to the absorption of energy from electrons provided by the filaments (Jia et al., 2010). In addition, pressure has been shown to affect film quality, boron-doping concentration, and diamond crystallographic plane growth direction (Jia et al., 2010). During the CVD diamond deposition process, the crystal morphology and orientation are directly related to the growth parameter, which specifies the ratio of the growth rates on different grain orientations [namely, between the (100) and (111) crystallographic planes for CVD diamond] (Lu X. R. et al., 2019). The growth parameter is mainly determined by different deposition parameters such as pressure, gas composition, and the temperature of the substrate (Wild et al., 1990; Wild et al., 1994; Paritosh et al., 1999; Tamor and Everson, 2011).

The choice of boron doping source and its concentration in the gas mixture significantly affect the BDD's molecular structure, electronic properties, composition, impurities, and direction of crystallographic diamond facets (Bogdanowicz and Ryl, 2022). The most used sources of boron in CVD diamond growth are gases such as trimethylborane [$B(CH_3)_3$], trimethylborate [$B(OCH_3)_3$], or diborane (B_2H_6). Solid-state sources such as boron oxide (B_2O_3) diluted in ethanol or methanol have also been successfully used (Brillas and Martínez-Huitle, 2011; Neto et al., 2016). Controlling the [B]/[C] ratio in the feed gas inside the reactor is established by determining appropriate mixing ratios based on Raoult's law (Einaga, 2018). Different boron sources may require different CVD growth conditions since boron incorporation depends on its source type. Gaseous boron precursors enable more precise control of the boron doping level over a wide concentration range (Cifre et al., 1994).

In addition to the commonly reported parameters, other factors related to the CVD reactor design and operation also affect the final characteristics of the BDD electrode. For example, the temperature measurement instruments and their position (thermocouple, pyrometer), the gas inlet point(s) in the reactor chamber, the direction of the gases' extraction, the chamber volume, or residence time of the gas mixture (depends on the chamber volume and gas flow/pressure). Slow cooling rates favor film adhesion due to lower residual stress caused by the CTE mismatch between the substrate material and the diamond film (Wei and Chen, 2008). The cooling atmosphere will also affect diamond surface chemical termination (Vanhove et al., 2007).

Both in-house and commercially made BDD electrodes show strong heterogeneities in their final characteristics due to the diverse deposition conditions and methods applied. The development of new technology or modified CVD reactors delivering homogeneous power into the diamond growth surface, together with selective BDD surface modifications, would be possible solutions to help minimize the currently found heterogeneities of BDD films (Bogdanowicz and Ryl, 2022).

4.3 Characterization of boron-doped diamond coatings

The microstructure, growth rate, sp^3/sp^2 ratio, boron doping level, and surface termination are key factors that determine the electrochemical properties of BDD. These characteristics significantly control their conductivity, OEP, electrochemical potential window, molecular adsorption, and electron transfer kinetics. Thus, a detailed characterization of a BDD film is also

an important point when comparing BDD electrodes from different sources.

In this section, the properties that most influence the electrochemical performance of the BDD electrodes will be discussed to better understand the efficiency of pollutants removal. The difficulty in comparing the diamond quality and boron doping levels in BDD thin films when determined by different characterization methods will also be addressed. One should bear in mind that the following considerations refer to BDD electrodes with planar geometry since distinct diamond-based architectures (e.g., BDD particles, nanostructured BDD, diamond-nanocarbon structures) may exhibit different behaviors (Baluchová et al., 2019; Bogdanowicz and Ryl, 2022).

4.3.1 Presence of non-diamond carbon

Raman spectroscopy is the most accepted and used technique for diamond quality assessment. It enables the detection of non-diamond carbon (NDC), allowing the determination of the carbon sp^3 (diamond-like)/sp^2 (graphite-like) ratio, which is the commonly adopted diamond quality indicator. The presence of NDC in the BDD films significantly influences their electrocatalytic properties, particularly the voltametric background current, potential window, molecular adsorption, and electron transfer kinetics (Macpherson, 2015). High NDC content affects the electrocatalytic inertia of the electrode (Macpherson, 2015) and modifies its adsorption characteristics, decreasing the potential window (Medeiros de Araújo et al., 2014) and increasing fouling susceptibility (Patel et al., 2013). Relevant presence of sp^2 carbon in the BDD films may induce voltametric responses like glassy carbon and graphite (He et al., 2019). The substantial presence of NDC in the grain boundaries of the diamond film causes lower electrode stability when under anodic polarization and, ultimately, the disintegration of the electrode (Read and Macpherson, 2016). The NDC content is also related to higher background current and double-layer capacitance (Bennett et al., 2004). For water treatment applications, a lower level of sp^2 carbon favors the ability for the mineralization of organics, and electrochemical combustion over conversion, thus avoiding the generation of hazardous by-products (Medeiros de Araújo et al., 2014).

Different laser wavelengths ranging from 257 to 1,064 nm have been used in Raman spectroscopy to evaluate the quality of the diamond thin films (Prawer and Nemanich, 2004). The determination of the sp^3/sp^2 ratio strongly depends on the excitation wavelength, and it increases with the increasing energy of the used laser (Prawer and Nemanich, 2004; Jagannadham et al., 2010). Typically, the peaks used for sp^3/sp^2 calculations are the first-order diamond band (sp^3) at 1,332 cm^{-1}; the G-band between 1,500 and 1,600 cm^{-1} (related to the C=C sp^2 bond stretching mode); and the D-band usually located at 1,345 cm^{-1} (represents most sp^2 structures) (Ballutaud et al., 2008; Dychalska et al., 2015). In the case of nanocrystalline diamond films, the first-order diamond peak is only detected under UV excitation (Prawer and Nemanich, 2004).

The comparison of different sp^3/sp^2 ratios is only accurate if the same excitation energy is used to acquire the spectra and if determined by the same method and mathematical expression. Several authors have used the ratio between the integral intensity of the diamond band ($I_{diamond}$) and the integral intensity of the G-band (I_G) (Isshiki et al., 2012). Others divide $I_{diamond}$ by the total integrated intensity of the Raman spectrum (I_{total}) (Salgueiredo et al., 2011; Štenclová et al., 2019). The full width at half maximum (FWHM) of the first-order peak for diamond has also often been used to estimate its crystalline quality and dopant concentration since lower FWHM values indicate lesser structural defects and/or grain boundaries, hence higher diamond quality (Gheeraert et al., 1993; Ferrari and Robertson, 2004; Prawer and Nemanich, 2004; Kowalska et al., 2020). Different expressions for the calculation of the diamond quality are found in the literature, depending on the applied excitation wavelength. For example, if the 514 nm excitation line is used, authors usually determine the diamond quality by Eq. 1 (Espinoza et al., 2019), Eq. 2 (McNamara et al., 1992), or Eq. 3 (Vorlíček et al., 1997).

$$sp^3 \Big/ sp^2\ ratio = \frac{I_{diamond}}{250 \times \sum I_{non-diamond}} \tag{1}$$

$$sp^3 \Big/ sp^2\ ratio = 100 \times \frac{I_G}{75 \times I_{diamond} + I_G} \tag{2}$$

$$\beta = \frac{I_{diamond}}{I_{diamond} + I_{total}} \tag{3}$$

In Eq. 1, $I_{non\text{-}diamond}$ is the integral intensity of non-diamond bands of the Raman spectrum, and 250 is the factor related to the Raman scattering efficiencies between the sp^3 band and other forms of non-diamond carbon. In Eq. 3, β is the figure-of-merit or the Raman quality fraction (Vorlíček et al., 1997). If the 488 nm excitation wavelength is used to acquire the Raman spectra, then the purity of the CVD diamond can be expressed by $C_{diamond}$, as seen in equation Eq. 4, where 50 is a correction factor for the substantial resonant Raman scattering effect of sp^2 bonded carbons (Shroder et al., 1990; Kowalska et al., 2020).

$$C_{diamond} = 100 \times \frac{I_{diamond}}{I_{diamond} + I_G/50} \tag{4}$$

It is important to emphasize that all the above equations for diamond quality assessment should be used with caution since several other factors influence the sp^3/sp^2 ratio. For instance, the polarization changes if micro or macro-Raman measurements are employed or if measurements are carried out over grains with different orientations (especially in micro-Raman) (Prawer and Nemanich, 2004).

4.3.2 Surface morphology and roughness

Scanning electron microscopy (SEM), atomic force microscopy (AFM), and 3D optical profilometry easily provide surface morphology and roughness analysis information. In polycrystalline BDD, the crystal defects are usually linked to NDC, mainly located in the grain boundaries. Therefore, higher surface roughness arises from large grain sizes and low grain boundary density, indicating a reduced amount of NDC present at the BDD surface (Williams, 2011; Gomez-Ruiz et al., 2019). Except in the case of UNCD films, CVD diamond films usually grow according to the van der Drift regime, in which the average grain size increases with the increasing film thickness (van der Drift, 1967). Therefore, grain size, roughness, and film thickness are closely related to the BDD surface's electrochemical properties, which, in their turn, are highly influenced by variation in the

amount of NDC. Consequently, the overpotential for oxygen evolution is lower for thinner films (and finer grains), and the capacitance of BDD electrodes is also related to surface roughness (Pleskov, 2011).

4.3.3 Boron doping level

The conversion of insulator diamond to metal-like conductivity is required for effective practical electrochemical applications and attained at certain doping levels (Yang et al., 2019). The evolution of resistivity in diamond as a function of boron concentration ([B]) in BDD thin films has been studied (Lagrange et al., 1998). For [B] bellow 10^{19} cm^{-3}, the conduction in diamond is dominated by free electrons within the valence band. Up to 3×10^{20} cm^{-3}, the conduction is of the hopping type, diamond behaves as a semiconductor, and the resistivity decreases strongly with the increase of boron content. Diamond reaches metal-like conductivity when [B] is above 3×10^{20} cm^{-3}.

Nevertheless, effective doping is not linear since boron does not homogeneously incorporate diamond, being simultaneously substitutional and interstitially distributed within the crystalline framework. Thus, effective boron doping does not linearly increase with the boost of boron concentration in the CVD feed gas (Sharma et al., 2022). Boron preferentially incorporates the (111) diamond facets compared to (100) facets (Spitsyn et al., 1981; Larsson, 2020). Electric conductivity in (111) planes is estimated to be approximately 10^4 times higher than that in (100) planes (Spitsyn et al., 1981), with consequent faster electron transfer kinetics in (111) planes (Bogdanowicz and Ryl, 2022). Furthermore, boron atoms are not electrically active when incorporated within the grain boundaries (Lu et al., 2012), which means that the measured doping level is usually higher than the effective carrier concentration (holes) (Yang et al., 2019). Several techniques have been used for quantitative and/or semiquantitative determination of the boron doping level in BDD films. It includes secondary ion mass spectrometry (SIMS), X-ray photoelectron spectroscopy (XPS), electron energy-loss spectroscopy (EELS), and neutron depth profile (NDP). However, these methods are time-consuming, expensive, and difficult to apply, especially when a full depth analysis of boron distribution within the diamond lattice is desired (Sharma et al., 2022). Recently, pulsed RF glow discharge optical emission spectroscopy (GDOES) has been used to semi-quantify boron doping levels, and it was demonstrated that the technique provides high-speed depth profiles (Sharma et al., 2022). In the case of heavily doped BDD films, many authors use a non-destructive and contactless measurement using Raman spectroscopy data to estimate the boron doping concentration. The following equation (Eq. 5) was proposed, and it is valid for boron doping concentration within the 2×10^{20} ~10^{22} cm^{-3} range (Bernard et al., 2004):

$$[B]\, cm^{-3} = 8.44 \times 10^{30} \exp\ (-0.048\omega) \tag{5}$$

where ω is the wavenumber (cm^{-1}) of the Lorentzian component of the Raman peak at about 500 cm^{-1}. Care must be taken when using this method since the intensity of the Raman peaks varies with the wavelength of the used laser (Prawer and Nemanich, 2004).

Understanding the electrical conductivity of BDD electrodes is complex and is not solely determined by the efficient amount of boron incorporation. Heterogeneities such as NDC content, lattice hydrogen, and dangling bonds also affect such property (Einaga et al., 2014). Enhanced BDD electrochemical performance is commonly linked to high boron doping levels, which provide higher carrier concentration and electrical conductivity (Einaga et al., 2014), thus electrochemical reactions are faster for heavier doped BDD electrodes (Pleskov, 2011). The doping level influence on the chemical surface of diamond electrodes was studied, and results indicate that highly doped diamond films show more reversible performances in the electrochemical response to the $Fe(CN)_6^{4-/3-}$ redox couple (Azevedo et al., 2013). Conversely, in the same study, other results indicate that increased doping level is associated with smaller grain size, with consequent increase of the grain boundary density that leads to a higher amount of NDC and surface oxidation states. The doping level effect of boron on the width of the electrochemical potential window of the electrodes revealed that low boron doping levels led to a broader potential range and slower response to the overpotential of both HER and OER (Salazar-Banda et al., 2010). This behavior is related to the minor concentration of boron-rich sites on the surface, blocking both hydrogen and oxygen adsorption steps required for HER and OER, respectively. Increasing boron content led to smaller electrochemical windows, as well as higher electron transfer rate constants and active electrochemical areas (Liu et al., 2018). Boron concentration also affects the adhesion strength of the film (Gerger and Haubner, 2008), diamond nucleation density, grain size, and overall diamond quality (Wang et al., 1992). Most published works on the electrochemical degradation of pollutants using BDD anodes do not provide information on effective boron content determination. In some cases, a rough estimative is expressed based on the [B]/[C] ratio in the feed gas during the CVD process. This estimate is inaccurate since boron incorporation in the diamond lattice is not linearly related to the feeding concentration, as previously demonstrated. An optimum balance between doping level and diamond quality must be reached to produce BDD electrodes with the desired and top electrochemical performance. Proper and accurate determination of the effective boron doping level is required to fine-tune the electrochemical properties of BDD films, although for practical applications the electrical conductivity can be used as a proxy for doping efficiency.

4.3.4 Surface termination

The surface termination of BDD electrodes can drastically influence their electrochemical kinetics (Yagi et al., 1999; Notsu et al., 2001). Hydrogen is the foremost gas used in the CVD growth of diamond films, and their surface presents a hydrogen-terminated surface if cooled down to room temperature under such flow. These surfaces are hydrophobic and show typical water contact angles around 90° (Neto et al., 2016). However, H-terminated diamond surfaces slowly oxidize with time when in contact with air, becoming more hydrophilic (Salazar-Banda et al., 2006; Vanhove et al., 2007). Several studies demonstrate that O-terminated BDD surfaces present a wider potential window, lower background current, and higher surface resistivity when compared to H-terminated surfaces (Yagi et al., 1999; Liu et al., 2007; Yano et al., 2019a; Yano et al., 2019b). Anodic polarization (Hutton et al., 2013) and oxygen plasma treatment are common means to obtain O-terminated BDD surfaces (Brillas and Martínez-Huitle, 2011). Oxidation of

the BDD surface can also be achieved by adding small amounts of O_2 or using an oxygen-containing boron source during the CVD deposition (Neto et al., 2016). The oxygen atoms incorporate the doped films by bonding with carbon atoms, mainly as C–O–C and C=O terminating groups (Neto et al., 2016). Evidence shows that increased boron doping levels lead to higher oxygen amounts with a consequent decrease in the water contact angle, showing a more hydrophilic character (Azevedo et al., 2013). O-terminated diamond surfaces show water contact angles ranging from 0.6° to 65° (Macpherson, 2015). The difference between H and O-terminated diamond surfaces is mainly associated with their electronic structures and surface bandgap (opposite bond polarities) (Liu et al., 2007). The former ($-C^{\delta-} - H^{\delta+}$) increases the energy levels of the valence (E_{VB}) and conduction bands (E_{CB}), as well as the negative electron affinity. The latter ($C^{\delta+} - O^{\delta-}$) lowers the energy levels and shows higher positive electron affinity (Macpherson, 2015).

The functional groups terminating the surface of BDD electrodes strongly influence the electron transfer kinetics of inner-sphere redox couples (Bard, 2010). The H-terminated BDD functional groups are usually $=CH_2$ and ≡C–H groups that, when oxidized under anodic polarization, show hydroxyl (≡C–OH), carbonyl (=C=O), carboxylic (–COOH), carbon radical ($\equiv C^{\bullet}$), and hydroxyl radical ($\equiv C-O^{\bullet}$) functional groups (Chaplin, 2014). These functional groups may vary according to the chosen anodic polarization procedure and the different grain orientations on the polycrystalline diamond surface (Yuan et al., 2021). Diamond surfaces with (111) orientation tend to be dominated by hydroxyl groups since only one chemical bond to a single carbon atom is available at the first surface layer. The latter then inhibits the formation of carbonyl and ether groups at the surface of the electrode (Chaudhuri et al., 2022). Diamond surfaces with (100) texture present two available chemical bonds for a single carbon atom, promoting carbonyl and ether group formation (Chaudhuri et al., 2022). For example, the $Fe(CN)_6^{4-/3-}$ redox system exhibits slow electron transfer for O-terminated surfaces but fast electron transfer for H-terminated surfaces (Yagi et al., 1999). In addition, H-terminated surfaces show narrower solvent potential windows than those O-terminated (Tryk et al., 2001).

Electrochemical pre-treatments and polishing have been carried out to enhance the BDD electroanalytical performance, increase the electrochemically active surface area, lower detection limits, and broader linearity ranges (Lourencao et al., 2020).

4.3.5 Electrochemical characterization

In a summarized way, the four main points to be taken into account in the electrochemical characterization of BDD electrodes are (Macpherson, 2015): good electrical contact to avoid ohmic drop effects, the cell apparatus, quantification of the capacitance and solvent potential window of the electrode, and assessment of the electron transfer kinetics with outer-sphere redox mediators.

Assessment of the solvent potential window is essential because it specifies the potential range over which the anode works prior to the electrolysis of the solvent (Macpherson, 2015). The electrochemical potential window will be the first quality indicator to be considered for the evaluation of the electrode performance, particularly if important information on the electrode is known (sp^3/sp^2 ratio, conductivity, surface termination, and morphology). The window range is pH-dependent and may vary depending on the electrolyte concentration, the electrode geometry, potential/current value, scan rate, and temperature. Electrolyte solutions commonly reported include KNO_3 (Yoon et al., 2012), H_2SO_4 (Kornienko et al., 2011), $HClO_4$ (Iniesta, 2001), Na_2SO_4 (Chen et al., 2022), NaBr, NaCl (Zhang et al., 2018), within a wide range of concentrations.

As already stated in the present review, the lack of information for comparison purposes includes the experiment temperature, whose increase leads to narrower electrochemical potential windows (McLaughlin et al., 2020). Another one is the adopted methodology regarding the determination of the solvent window (from the voltammogram), which is commonly carried out by applying a method based on defining the window at an arbitrary current density cut-off ($J_{cut-off}$) value or a linear fit method (Olson and Bühlmann, 2012). The arbitrary method is highly influenced by the mass transport of the electrolyte (McLaughlin et al., 2020), and the setting of $J_{cut-off}$ values has been diversely defined in the literature, limiting possible comparison of the obtained results (Mousavi et al., 2015). On the other hand, the linear fit method is less affected by the experimental conditions for each measurement system, becoming the recommended one for accurately comparing solvent potential windows (McLaughlin et al., 2020).

The OEP of an electrode material and the enthalpy of adsorption of the hydroxyl radicals on its surface are the main factors that determine its oxidation power (Comninellis et al., 2008). This parameter is simple to obtain, it is also a good indicator of electrode quality, and it should be carefully evaluated. OEP determines if the anode presents an active or a non-active behavior (Comninellis et al., 2008). Usually, BDD is considered a non-active anode due to its high OEP, which indicates a more significant restriction of the oxygen evolution from water electrolysis and the production of hydroxyl radicals at the surface of the electrode (Lee et al., 2017). Comparison of OEP values is only valid if obtained for the same solution concentration and electrolyte.

Determination of the double-layer capacitance (C_{dl}) is also a helpful indicator of electrode quality (Macpherson, 2015). C_{dl} can be calculated from cyclic voltammetry applying Eq. 6 or through electrochemical impedance spectroscopy (EIS) measurements.

$$C_{dl} = \frac{i_{av}}{A\nu} \tag{6}$$

where i_{av} is the average current from the forward and reverse sweep, A is the electroactive area, and ν is the scan rate. Nevertheless, the application of this equation becomes challenging due to the topographic nature of the BDD surface (especially in MCD), which restricts the accurate determination of the electroactive area (Macpherson, 2015).

The electron transfer kinetics may be evaluated from cyclic voltammogram measurements for inner-sphere and outer-sphere redox couples. The most studied redox couples are the inner-sphere $Fe(CN)_6^{-3/-4}$ and the outer-sphere $Ru(NH_3)_6^{3+/2+}$ redox couples. The latter is valuable for qualitative estimation of the boron doping level. BDD films with a dominant electrical transport mechanism (i.e., metal-like conductivity) show a reversible or quasi-reversible faradaic peak current response under conditions where the electron transfer rate is much faster than the diffusional rate (Macpherson,

TABLE 3 Accelerated life test results and experimental conditions found for several studied BDD electrodes.

Electrolyte	Substrate material	Current density (A/cm^2)	Accelerated life test result (h)	Ref.
0.5 M H_2SO_4	Nb	10	850	Fryda et al. (1999)
1 M H_2SO_4	Nb	1.32	88–130	Choi et al. (2017)
		1	484	Lu et al. (2019a)
	Si	1	262	Miao et al. (2020)
	Ti	1	127	Lu et al. (2018), Lu et al. (2019b)
3 M H_2SO_4	Nb	1	>1,600	Yang et al. (2022)
	Si	1	>1,600	Yang et al. (2022)
	Ta	1	>1,600	Yang et al. (2022)
	Ti	1	1,530	Yang et al. (2022)
		1	264	Chen et al. (2005)
		1	95	Chen and Chen (2004)
		0.5	89	He et al. (2015)
6 M HNO_3	Nb	0.5	1,620–1810	Groenen Serrano et al. (2015)

2015). However, the oxidation and reduction reaction rate of $Ru(NH_3)_6^{2+/3+}$ is little affected by surface defects, film microstructure, adsorbed sp^2 carbon, or surface terminations like oxygen-containing groups (Ueda et al., 2009; Dettlaff et al., 2021). On the contrary, the $Fe(CN)_6^{3-/4-}$ redox couple electron transfer rate is significantly affected by the surface chemistry of the BDD coating and the presence of defects such as NDC impurities (Dettlaff et al., 2021).

4.3.6 Electrode service life

Ultimately, comparing the service time of different BDD electrodes is equally important to balance performance and lifetime service with optimal cost-benefit in large-scale water treatment applications. Accelerated life tests are a practical way of evaluating the BDD's electrochemical stability over time (Zhang C. et al., 2019). Accelerated service life tests have been performed on BDD films deposited over various substrate materials (*e.g.*, Nb, Si, Ti, Ta) through electrolysis at high current densities ranging from 0.5 to 10 A/cm^2 in concentrated electrolyte solutions of H_2SO_4 or HNO_3. Table 3 shows the accelerated life tests and their experimental conditions found in the literature.

4.4 Design of pollutant degradation experiments

The mineralization efficiency is influenced by the applied current density, EAOP, pollutant concentration, properties of the degraded pollutant, pH of the solution, supporting electrolyte, temperature, the volume of solution, fluid dynamics, dissolved oxygen, electrode configuration, active electrode area, cell design, and agents added in the solution, e.g., chloride, sulfate, phosphate, carbonate, and oxygen (Brillas et al., 2005; Enache et al., 2009; Panizza and Cerisola, 2009; Macpherson, 2015; Cano et al., 2016; Rubí-Juárez et al., 2016; Xu, 2016; McLaughlin et al., 2020). Comparing the degradation performance of BDD electrodes is again a repetitive challenge.

4.4.1 Electrochemical advanced oxidation process

In EAOPs, the primary processes are classified as anodic oxidation (AO) *via* intermediates of oxygen evolution and electro-Fenton-based processes. Anodic oxidation *via* intermediates (hydroxyl radicals formed from water oxidation at the anode surface) resulting from oxygen evolution may directly destroy organic pollutants (Belhadj Tahar and Savall, 2019). Electrogeneration of H_2O_2, denominated AO with electrogenerated H_2O_2 (AO-H_2O_2), is another anodic oxidation method (Brillas et al., 2008). The efficiency of both methods depends on the type of material used as anode and must present high OEP (Moreira et al., 2017). Anodic oxidation can also be accomplished by adding anions to the bulk solution, such as chloride, sulfate, phosphate, and carbonate, that generate oxidants like active chlorine, persulfate, perphosphate, and percarbonate species, respectively (Panizza and Cerisola, 2009). The electro-Fenton (EF) process arises from the electrochemical production of H_2O_2 with the addition of Fe^{2+} in the bulk solution producing additional hydroxyl radicals as a by-product of the Fenton's reaction (Brillas et al., 2004). Photoelectro-Fenton (PEF) and solar photoelectro-Fenton (SPEF) are a combination of the EF method with the irradiation of UV light and natural sunlight, respectively, that enhance degradation efficiency (Brillas, 2014). The sonoelectro-Fenton (SEF) process is performed under EF conditions and simultaneous application of ultrasound radiation (Oturan et al., 2008). Electrochemical degradation experiments combining UV or ultrasound irradiation demonstrated improved outcomes if compared to direct anodic oxidation (Hurwitz et al., 2014; Vidales et al., 2014; Vieira Dos Santos et al., 2017). Ultrasound radiation improves the transfer of pollutants to the BDD surface though it requires higher energy consumption; and UV irradiation increases hydroxyl radical generation (Vidales et al., 2014),

preventing the formation of undesirable and hazardous by-products (e.g., chlorate and perchlorates) during the electrochemical degradation process (Cotillas et al., 2016). The key EAOPs are AO, AO-H_2O_2, EF, PEF, and SPEF (Sires et al., 2014). Other EAOPs such as peroxi-coagulation (Brillas and Casado, 2002) and Fered-Fenton (Huang et al., 2001) are also proposed for remediation of various pollutants in wastewater.

The main disadvantages of EAOPs are high energy consumption and mandatory solution high conductivity which is directly correlated to lower energy conditions (Clematis and Panizza, 2021b). The effluents from several industries and urban wastewater have low conductivities, but adding a supporting electrolyte enables water treatment by direct application of electrochemical processes (Ma et al., 2018). Still, this extra leads to increased operational costs and/or toxic by-products (Clematis and Panizza, 2021b). Alternatives include reduction of ohmic resistances and increasing the mass transport of the pollutants towards the surface of the electrode through a solid polymer electrolyte (SPE) (Clematis et al., 2017), or capillary microfluidic cells (Ma et al., 2018), respectively. A review on the electrochemical oxidation of organic pollutants in low conductive solutions can be found elsewhere (Clematis and Panizza, 2021b).

4.4.2 Cell design

Various configurations and apparatus have been used in pollutant degradation with BDD electrodes, including simple electrochemical cells under static conditions and commercial multi-cell flow reactors. Thus, the influence of the electrode configuration and cell design on the intrinsic fluid dynamics (e.g., volumetric flow, Reynolds number, and mass transport) is an important factor (Cano et al., 2016; Xu, 2016).

Cells are usually equipped with two types of electrode configurations: monopolar and bipolar designs (Cano et al., 2016). In the first one, the anode is BDD, and the cathode is another material, usually a stainless-steel plate. In bipolar design, BDD is used as both anode and cathode. Both configurations under the same operating conditions were tested, and the bipolar electrodes provided higher efficiency in water disinfection (Cano et al., 2016). Moreover, reactors designed for cells with bipolar configuration allow switching the polarity of electrodes to electrochemically clean their surface and prevent electrode deactivation (Murugananthan et al., 2007). Nevertheless, one should bear in mind that monopolar electrodes consume less energy (Cano et al., 2016).

The type and geometry of the cell and the BDD electrodes are essential aspects since they will determine the flow dispersion and consequent mass transport within the container. The latter will directly influence the potential and current distribution of the working electrode, affecting the current efficiency and overall energy consumption associated with the degradation process (Rivera et al., 2015; Cornejo et al., 2020).

4.4.3 Operating conditions

According to the literature, the adopted operating conditions to perform electrochemical oxidation of contaminants in wastewater are diverse. However, the removal of organic carbon from treated solutions is mainly influenced by the applied current density, mass transfer effects, and the properties of degraded pollutants (Xu, 2016).

Many degradation experiments are performed with the addition of a supporting electrolyte, particularly in high concentrations (higher solution conductivity) where electrooxidation proficiency is enhanced (Ma et al., 2018). The effect of different supporting electrolytes in phenol degradation using BDD electrodes has been assessed (de Souza and Ruotolo, 2013). In the absence of chloride ions, the oxidation kinetics constants follows the order: $Na_2SO_4 \approx Na_2CO_3 > H_2SO_4 > H_3PO_4$. In chloride-mediated process, the reaction kinetics considerably increases with a new order: $H_2SO_4 > Na_2SO_4 > Na_2CO_3$. Therefore, the supporting electrolyte plays a crucial role in generating different oxidative species like peroxocarbonate, peroxosulfate, or hypochlorite (Rubí-Juárez et al., 2016). The choice of electrolyte will affect the pH value, and acidic media is correlated to the improvement of pollutant degradation efficiency, benefiting the production of hydroxyl radicals at the anode surface (Zhou et al., 2011a; Daskalaki et al., 2013; Espinoza-Montero et al., 2013; Fabianska et al., 2014). However, in terms of pH effect, there are diverse and even contradictory results which are dependent on the pollutant chemistry (Brillas et al., 2005; Zhou et al., 2011b; Xu, 2016). Ideally, the electrochemical behavior of BDD electrodes should be evaluated in different pH and electrolyte solutions before the degradation experiments (Enache et al., 2009).

Mineralization rates are linearly related to the current density (j_{appl}) with two different operating regimes depending on it: current and mass transport-controlled oxidations (Brillas et al., 2005). In these regimes, the limiting current density (j_{limit}) for electrooxidation of the organic pollutant is estimated according to the following equation:

$$j_{limit} = n k_m F [Pollutant] = 4 k_m F COD \quad (7)$$

where j_{limit} is the limiting current density, [Pollutant] is the organic pollutant concentration, k_m is the mass-transfer coefficient, n is the number of electrons exchanged in the oxidation of a molecule of the pollutant, F is the Faraday constant, and COD is the chemical oxygen demand. Current-controlled oxidation takes place when $j_{appl} < j_{limit}$, and the contaminant concentration decreases linearly over time with a current efficiency of 100% (Panizza et al., 2001). On the other hand, mass transport-controlled oxidation occurs when $j_{appl.} > j_{limit}$, and secondary reactions like oxygen evolution occur. In this case, the contaminant degradation follows an exponential trend, and the current efficiency is below 100% (Panizza et al., 2001).

The geometric area of the BDD anode should be controlled since its conductivity is not entirely uniform along with the film due to its surface heterogeneities. Restricted areas prevent poor current density distribution and, consequently, lower degradation efficiency and possible formation of undesired by-products (Cano et al., 2016). The relationship between the electrode area and the applied current density is meaningful: the same degradation performance with a reduced electrode area is achieved by increasing the current density. Its maximum is defined by the quality, defect density, and adhesion strength of the BDD film to the substrate. Still, lower current densities may avoid the production of non-desired or hazardous by-products (chlorate, perchlorate, or organo-chlorinates) (Cano et al., 2011).

The total volume of solution affects the residence time and, consequently, the degradation efficiency (Lacasa et al., 2013). In addition, high pollutant concentration leads to lower mineralization rates but higher temperature promotes faster mineralization rates due to further mass transfer towards the anode surface (Brillas et al., 2005).

4.4.4 Performance indicators for pollutant degradation

The measurement of COD in the solution containing the contaminant under study is the most applied approach to assess the degradation performance of BDD electrodes. Some authors also evaluate the total organic carbon (TOC) of the solution, or both COD and TOC, and others prefer to express degradation results as a function of the contaminant concentration. The latter is usually determined by UV-vis spectroscopy and/or high-performance liquid chromatography (HPLC).

The COD method is used to quantify the performance of the electrodes. It determines the average current efficiency (ACE) and instantaneous current efficiency (ICE) of the BDD electrode, expressed in Eqs 8, 9, respectively (Comninellis and Pulgarin, 1991):

$$ACE = \frac{F\,V\,(COD_0 - COD_t)}{8\,I\Delta t} \tag{8}$$

$$ICE = \frac{F\,V\,(COD_t - COD_{t+\Delta t})}{8\,I\Delta t} \tag{9}$$

where F is the Faraday constant (96485 C mol^{-1}); t is the time s); V is the volume of the electrolyte (dm^3); COD_0 is the initial COD concentration (g_{O2} dm^{-3}); COD_t and $COD_{t+\Delta t}$ are the COD concentration at times t and t+Δt (s), respectively; I is the applied current (A); and 8 is the dimensional factor for unit consistency (meaning 32 g of O_2/4 mol e^- mol^{-1} of O_2).

Likewise, current efficiency results have also been measured as a function of TOC. For example, the mineralization current efficiency (MCE) is calculated considering TOC removal (Eq. 10) (Flox et al., 2007). In addition, the combustion efficiency (Eq. 11) can be determined by calculating the ratio between the TOC and the COD decrease rates (Pacheco et al., 2007):

$$MCE = \frac{n\,F\,V\Delta TOC}{4.32 \times 10^7 m\,I\,t} \tag{10}$$

$$\eta_c = \frac{32}{12}\left(\frac{n}{4m}\right)\frac{dTOC}{dCOD} \tag{11}$$

where n is the number of electrons required for the complete combustion of the organic pollutant, m is the number of carbon atoms in the molecule of the organic pollutant, F is the Faraday constant, V is the volume of the electrolyte (L), I is the applied current (A), t is the time (h), ΔTOC is the total organic carbon reduction (mg/L), dTOC is the TOC decrease rate, and dCOD is the COD decrease rate.

If the concentration of the pollutant is evaluated over its electrooxidation time, the results are usually demonstrated in plots of removal percentage, or contaminant concentration, against the charge amount Q^t (Eq. 12).

$$Q^t\ (Ah/L) = \frac{\mathrm{jAt}}{V} \tag{12}$$

However, Q^t does not consider the total removed concentration of the pollutant from the solution. Therefore, we propose a different approach to determine the degradation performance, which enables comparison between the reported results. It starts by calculating the average Q′ (Ah/kg) required for the pollutant degradation, expressed through Eq. 13.

$$Q'\left(Ah/kg_{pollutant}\right) = Q^t \times \frac{1}{\Delta C_{pollutant}} = \frac{\mathrm{jAt}}{V\Delta C_{pollutant}} \tag{13}$$

We propose Q′, a new figure-of-merit to be used when COD and TOC are undetermined and the cell potential value is unavailable, i.e., when the calculation of energy consumption is not possible. Q′ is a base parameter to enable comparison between different performances of the BDD electrodes from different sources (in-house and commercially manufactured). Energy consumption values have been reported in several ways as a function of the removed concentration of the studied analyte (Eq. 14), COD (Eq. 15), and TOC (Eq. 16). Additionally, some authors have expressed energy consumption values only as a function of the volume of the treated solution (Eq. 17). However, the latter expression of consumption does not consider the pollutant concentration and may induce misinterpretation of the electrode performance.

$$Energy\ consumption\left(\frac{kWh}{kg_{pollutant}}\right) = Q^t \times \frac{E}{\Delta C_{pollutant}} = \frac{\mathrm{EjAt}}{V\Delta C_{pollutant}} \tag{14}$$

$$Energy\ consumption\left(\frac{kWh}{kg_{COD}}\right) = Q^t \times \frac{E}{\Delta COD} = \frac{\mathrm{EjAt}}{V\Delta COD} \tag{15}$$

$$Energy\ consumption\left(\frac{kWh}{kg_{TOC}}\right) = Q^t \times \frac{E}{\Delta TOC} = \frac{\mathrm{EjAt}}{V\Delta TOC} \tag{16}$$

$$Energy\ consumption\ (kWh/m^3) = Q^t \times E = \frac{\mathrm{EjAt}}{V} \tag{17}$$

where Q^t is the charge (Ah/dm^3) at time t (h), j is the applied current density (A dm^{-2}), t is the electrolysis time (h), A is the BDD electrode geometric area (dm^2), V is the volume (dm^3) of the solution, E is the average electrode potential (V), $\Delta C_{pollutant}$ is the total concentration of pollutant removed from the solution (kg/dm^3), ΔCOD is the total amount of COD removed (kg/dm^3), and ΔTOC is the total amount of TOC removed (kg/dm^3).

The previous equations allow normalization of the BDD degradation results for a specific contaminant (Eq. 14) or complex matrixes (Eqs 15, 16) based on diverse experimental conditions like applied current density, electrode potential, geometric electrode area, degradation time, the volume of solution, and initial pollutant concentration. Although one may use such figures-of-merit, understanding the different results is only achieved through proper and complete characterization of the BDD films, as discussed in the previous sections. In addition, a comparison of the results is only possible within each specific calculation method. For example, the COD method (ICE, ACE, energy consumption in kWh/kg_{COD}), TOC (MCE, η_c, energy consumption in kWh/kg_{TOC}), and pollutant concentration (Q′, and energy consumption in $kWh/kg_{pollutant}$). A summary of the figures of merit discussed in this section is provided in Table 4.

TABLE 4 Summary of figures of merit used as performance indicators for pollutant degradation.

Figure-of-merit (FOM)	Pros	Cons
$ACE = \frac{F\,V\,(COD_0 - COD_t)}{8\,I\Delta t}$	Most used FOMs, allowing comparison with most published results COD measurements are less expensive than TOC	Does not give information on the oxidation of a specific pollutant The COD analysis uses hazardous reagents (dichromate), can be time-consuming, have a relatively high detection limit, and may suffer interference from inorganics. In addition, dichromate does not oxidize some organic species, which can imply false low COD values
$EC_{COD} = \frac{EjAt}{V\Delta COD}$		
$ICE = \frac{F\,V\,(COD_t - COD_{t+\Delta t})}{8\,I\Delta t}$	Provide instantaneous current efficiency data	
$MCE = \frac{n\,F\,V\Delta TOC}{4.32 \times 10^7\, m\,I\,t}$	TOC analyses are usually faster than COD and often result in accuracy over an extensive range of concentrations from 1 to 50,000 ppm	TOC measurements require expensive equipment and complicated analysis
$EC_{TOC} = \frac{EjAt}{V\Delta TOC}$		
$\eta_c = \frac{32}{12}\left(\frac{n}{4m}\right)\frac{dTOC}{dCOD}$		Requires both COD and TOC measurements
$Q' = \frac{jAt}{V\Delta C_{pollutant}}$	Ideal for comparing results when the cell potential value is unavailable Does not require COD and/or TOC analysis	Requires pollutant quantification techniques (e.g., UV-vis spectroscopy, HPLC)
$EC_{Pollutant} = \frac{EjAt}{V\Delta C_{pollutant}}$	Does not require COD and/or TOC analysis	
$Q^t = \frac{jAt}{V}$	Does not require quantification methods (e.g., pollutant concentration, COD or TOC)	Does not consider the pollutant concentration or any other water quality parameter, which may lead to misinterpretation
$EC_{Volume} = \frac{EjAt}{V}$		

*EC, energy consumption.

5 Case studies and comparisons according to the literature

There are only a few studies comparing in-house electrodes with commercial ones (Hutton et al., 2013; Huang et al., 2021). For example, eleven different BDD electrodes over Nb substrates by HFCVD were produced by varying the $B(OCH_3)_3/CH_4$ gas mixture (0.125%–0.75%), CH_4/H_2 ratio (0.5%–1.0%), and gas pressure (5–15 torr) (Huang et al., 2021). They were then compared to commercial BDDs manufactured by Neocoat and Diachem in terms of electrochemical degradation of guaifenesin (pharmaceutical) and TOC removal. Four in-house prepared BDD electrodes showed more significant OEP values reaching a value of 2.45 V against 2.36 V (vs. Ag/AgCl) (commercial). The in-house electrodes [$B(OCH_3)_3/CH_4$ ratio of 0.75%, CH_4/H_2 ratio of 1%, 5 torr pressure] exhibited the second-best performance in terms of electrochemical degradation of the contaminant as well as TOC removal. The best-performance in-house produced electrode showed a pseudo-first-order reaction rate constant for guaifenesin degradation of 0.33 min^{-1}, compared to 0.35 min^{-1} (Neocoat) and 0.27 min^{-1} (Diachem). After 120 min of electrolysis, the TOC removal efficiency was 100% for the in-house electrode, 100% for Neocoat and 97% for Diachem. Thus, in-house produced BDD anodes may exhibit similar or even superior performance than commercial ones. However, for such statement it is necessary to ensure that the electrodes performance data are reliable and statistically relevant.

According to SLR, phenol and landfill leachate appeared as the analytes with the highest occurrence among articles that use BDD electrodes for electrochemical degradation of water pollutants. In this section, we will discuss most of the published results (to the best of our knowledge) and the diversity of operating conditions when degrading spiked solutions with phenol (Supplementary Table S4) or treating landfill leachate (Supplementary Table S5). One should note that the information included in the previous tables only relates to results obtained using planar BDD electrodes under the simplest operating conditions for each published article. Moreover, when results were absent along the text and tables of the analyzed articles, data was extracted from plotted graphs using the WebPlotDigitizer tool (Rohatgi, 2019).

The operating conditions used for the electrochemical treatment of phenol and landfill leachate are diverse. In the case of phenol (Supplementary Table S4), ACE values range from 12.3% to 87%, and energy consumption from 26.6 to 475 kWh/kg_{COD}. The average ACE for in-house electrodes is 32.4%, against 44% for commercial electrodes. Energy consumption data is insufficient to establish further comparisons since it is presented in different units (e.g., kWh/kg_{COD}, kWh/kg_{TOC}, $kWh/kg_{phenol,}$ and kWh/m^3). Overall data analysis indicate that commercial electrodes appear to consume less energy and present better current efficiency for phenol degradation. Nevertheless, it is impossible to unambiguously confirm this trend due to the different operating conditions and configuration variability of the electrodes and reactors.

Considering landfill leachate treatment (Supplementary Table S5), ACE values range from 14.4% to 193%, and energy consumption from 5.7 to 285 kWh/kg_{COD}. Disregarding experimental conditions, in-house electrodes present higher ACE values but higher energy consumption when compared to commercial ones. Again, one should note that the operating conditions are significantly divergent, and that landfill leachates are complex and variable mixtures that may interfere with synergistic or antagonistic effects.

This review largely reflects the significant variability within the results and the influence of several parameters on the performance of the BDD electrodes (summarized in Figure 8). Considering the few possible comparisons withdrawn in this work, it is not possible to conclude which electrode would be the best choice. Such decision highly depends on proper and effective comparisons under the same degradation conditions and electrochemical cell configuration for a wide range of model pollutants and real wastewater systems. Only then it will be possible to properly evaluate and compare in-house electrodes with commercial ones.

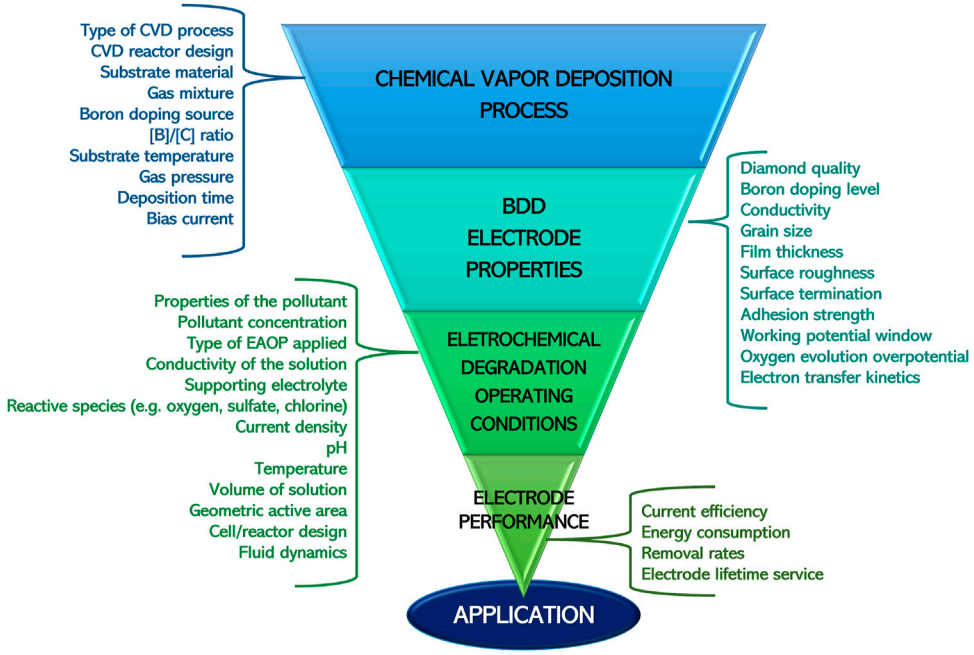

FIGURE 8
Main factors influencing the performance of BDD electrodes in the electrochemical degradation of pollutants (source: the authors).

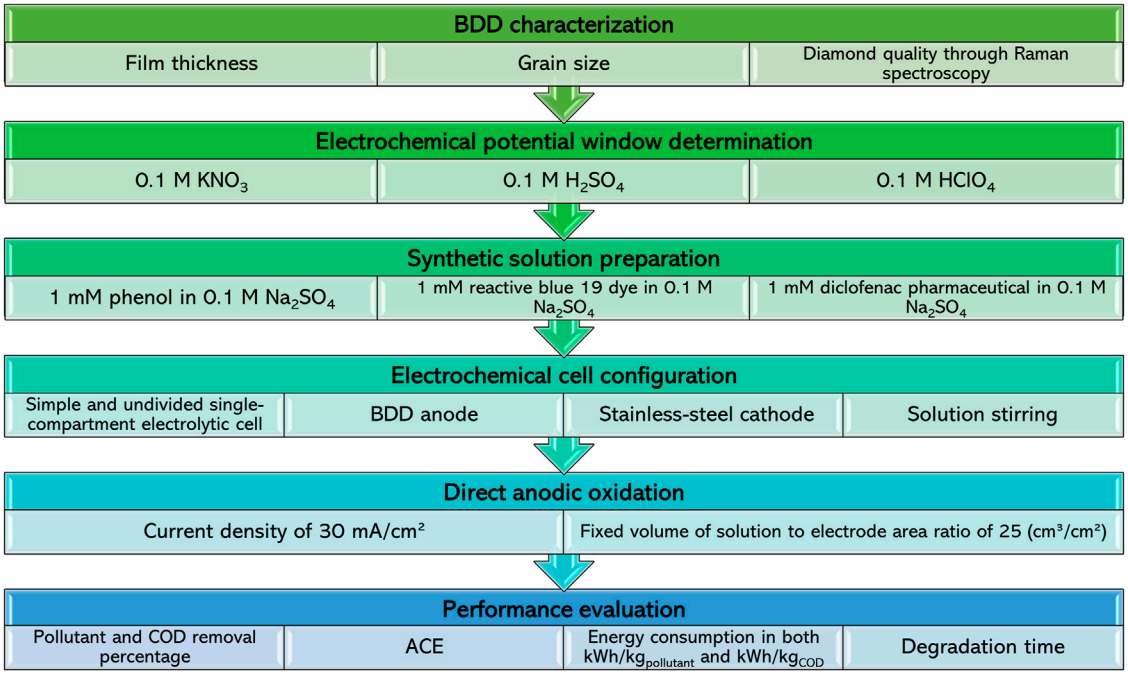

FIGURE 9
Experimental procedure proposed for evaluating BDD electrodes (source: the authors).

6 Critical perspectives and future outlook

In this critical review, a detailed discussion of the most relevant parameters that influence the performance of BDD electrodes in the electrooxidation of water pollutants was carried out. The SLR and bibliometric network graphs were valuable tools to identify the most studied water pollutants, applied EAOPs, and relevant issues such as energy consumption, by-products and toxicity of the treated waters. Based on the gathered information, an attempt was made to

compare the electrooxidation performance between in-house and commercially available BDD electrodes. Both types of electrodes show strong heterogeneities in their final physicochemical characteristics due to the diversity of deposition conditions and applied methods. The comparison attempt is further complicated by the variety of methods, parameters, or electrochemical cells used in the pollutant degradation experiments. Due to the lack of essential information for such comparison, it is not possible to state which one would be the best.

Over the years, many different figures-of-merit based on COD, TOC, or the concentration of the pollutant studied, have been proposed to determine the performance of BDD electrodes. Here, we propose a figure-of-merit equation which normalizes BDD degradation results for a specific contaminant, even if working under different experimental conditions like applied current density or initial pollutant concentration. This is however a remedial solution to allow comparing data obtained under very different conditions.

Data analysis for phenol degradation and landfill leachate treatment generally suggest that commercial BDD electrodes appear to consume less energy and present better current efficiency than in-house prepared anodes. These indications are subjective to a certain point since there is significant variability in the reported operating conditions, which precludes unequivocal conclusions to be made. Nevertheless, there is a strong indication that if in-house electrodes are further optimized, they could reach or surpass the performance of those commercially available. This analysis also points ways for these companies to improve the efficiency of their products.

Our suggestion is to create a uniform reporting/testing procedure: authors could provide further details on the produced BDD electrodes (film thickness, grain size, diamond quality through Raman spectroscopy, resistivity, and working potential window) in three model electrolytes (e.g., 0.1 M KNO_3, 0.1 M H_2SO_4, and 0.1 M $HClO_4$). Based on the case study of phenol, we further suggest that all laboratories could perform three water electrooxidation tests, each one with a different model pollutant (e.g., phenol, reactive blue 19 dye, diclofenac pharmaceutical), through direct anodic oxidation in an undivided single-compartment electrolytic cell, under constant stirring, using a BDD anode and a stainless-steel cathode (same geometric area). Moreover, a pollutant concentration of 1 mM, applied current density of 30 mA/cm^2, electrolyte solution of Na_2SO_4 for fixing solution conductivity and pH, and a fixed volume of solution to electrode area ratio of 25 (cm^3/cm^2) should be adopted. The degradation results should be compared as a function of pollutant and COD removal percentage, ACE, energy consumption (in $kWh/kg_{pollutant}$ and kWh/kg_{COD}), and degradation time. The proposed procedure is summarized in a flowchart (Figure 9).

Ideally, a standard or normalized procedure should be elaborated, bringing the scientific community and manufacturers together to discuss and reach a consensus on the best practices to evaluate and compare the electrooxidation performance of a BDD electrode, independently of their origin. The creation of such consensual standard would enable faster developments and a straightforward transition of in-house BDD electrodes to commercial production with consequent effective large-scale application in water treatment plants.

Author contributions

Conceptualization: FO and PB; investigation: PB; writing-original draft preparation: PB; writing-review and editing: AG; supervision: FO and JT; project administration: FO and RS; funding acquisition: RS. All authors have read and agreed to the published version of the manuscript.

Funding

This work was developed within the scope of the project CICECO-Aveiro Institute of Materials, UIDB/50011/2020, UIDP/50011/2020, and LA/P/0006/2020, financed by national funds through the FCT/MEC (PIDDAC). This work is also funded by national funds (OE) through FCT—Fundação para a Ciência e a Tecnologia, I.P., in the scope of the framework contract foreseen in the numbers 4, 5, and 6 of the article 23, of the Decree-Law 57/2016, of 29 August changed by Law 57/2017, of 19 July.

Acknowledgments

The authors wish to thank the University of Aveiro and CICECO—Aveiro Institute of Materials for their contributions to this work, as well as the organizations responsible for funding the project: European Regional Development Fund (FEDER) and Fundação para a Ciência e a Tecnologia (FCT).

Conflict of interest

The authors declare that the research was conducted in the absence of any commercial or financial relationships that could be construed as a potential conflict of interest.

Publisher's note

Supplementary material

The Supplementary Material for this article can be found online at: https://www.frontiersin.org/articles/10.3389/fmats.2023.1020649/full#supplementary-material

References

Alvarez Pugliese, C. E., Martínez Hernández, L., Imbachi Ordoñez, S., Marriaga Cabrales, N., and Machuca Martínez, F. (2016). Pilot scale anodic oxidation of pretreated vinasse using boron doped diamond electrodes. *CT&F - Cienc. Tecnol. Futuro* 6 (4), 67–77. doi:10.29047/01225383.04

Araújo, C. A. Á. d. (2006). Bibliometria: Evolução histórica e questões atuais. *Em Questão* 12 (1), 11–32.

Azevedo, A. F., Baldan, M. R., and Ferreira, N. G. (2013). Doping level influence on chemical surface of diamond electrodes. *J. Phys. Chem. Solids* 74 (4), 599–604. doi:10.1016/j.jpcs.2012.12.013

Ballutaud, D., Jomard, F., Kociniewski, T., Rzepka, E., Girard, H., and Saada, S. (2008). Sp3/sp2 character of the carbon and hydrogen configuration in micro- and nanocrystalline diamond. *Diam. Relat. Mater.* 17 (4-5), 451–456. doi:10.1016/j.diamond.2007.10.004

Baluchová, S., Taylor, A., Mortet, V., Sedláková, S., Klimša, L., Kopeček, J., et al. (2019). Porous boron doped diamond for dopamine sensing: Effect of boron doping level on morphology and electrochemical performance. *Electrochimica Acta* 327, 135025. doi:10.1016/j.electacta.2019.135025

Bard, A. J. (2010). Inner-sphere heterogeneous electrode reactions. Electrocatalysis and photocatalysis: The challenge. *J. Am. Chem. Soc.* 132 (22), 7559–7567. doi:10.1021/ja101578m

Belhadj Tahar, N., and Savall, A. (2019). Mechanistic aspects of phenol electrochemical degradation by oxidation on a Ta/PbO2 anode. *J. Electrochem. Soc.* 145 (10), 3427–3434. doi:10.1149/1.1838822

Bennett, J. A., Wang, J., Show, Y., and Swain, G. M. (2004). Effect of sp[sup 2]-bonded nondiamond carbon impurity on the response of boron-doped polycrystalline diamond thin-film electrodes. *J. Electrochem. Soc.* 151 (9), E306–E313. doi:10.1149/1.1780111

Bergmann, M. E. H., Iourtchouk, T., Schmidt, W., Hartmann, J., Fischer, M., Nüsske, G., et al. (2015). Laboratory- and technical-scale comparison of chlorate and perchlorate formation during drinking water electrolysis: A field study. *J. Appl. Electrochem.* 45 (7), 765–778. doi:10.1007/s10800-015-0826-z

Bernard, M., Deneuville, A., and Muret, P. (2004). Non-destructive determination of the boron concentration of heavily doped metallic diamond thin films from Raman spectroscopy. *Diam. Relat. Mater.* 13 (2), 282–286. doi:10.1016/j.diamond.2003.10.051

Bogdanowicz, R., and Ryl, J. (2022). Structural and electrochemical heterogeneities of boron-doped diamond surfaces. *Curr. Opin. Electrochem.* 31, 100876. doi:10.1016/j.coelec.2021.100876

Braga, N. A., Cairo, C. A. A., Matsushima, J. T., Baldan, M. R., and Ferreira, N. G. (2009). Diamond/porous titanium three-dimensional hybrid electrodes. *J. Solid State Electrochem.* 14 (2), 313–321. doi:10.1007/s10008-009-0855-9

Brillas, E., Boye, B., Sirés, I., Garrido, J. A., Rodrı´guez, R. M. a., Arias, C., et al. (2004). Electrochemical destruction of chlorophenoxy herbicides by anodic oxidation and electro-Fenton using a boron-doped diamond electrode. *Electrochimica Acta* 49 (25), 4487–4496. doi:10.1016/j.electacta.2004.05.006

Brillas, E., and Casado, J. (2002). Aniline degradation by Electro-Fenton® and peroxi-coagulation processes using a flow reactor for wastewater treatment. *Chemosphere* 47 (3), 241–248. doi:10.1016/s0045-6535(01)00221-1

Brillas, E. (2014). Electro-fenton, uva photoelectro-fenton and solar photoelectro-fenton treatments of organics in waters using a boron-doped diamond anode: A review. *J. Mexican Chem. Soc.* 58 (3), 239–255. doi:10.29356/jmcs.v58i3.131

Brillas, E., Garrido, J. A., Rodríguez, R. M., Arias, C., Cabot, P. L., and Centellas, F. (2008). Wastewaters by electrochemical advanced oxidation processes using a BDD anode and electrogenerated H2O2 with Fe(II) and UVA light as catalysts. *Port. Electrochimica Acta* 26 (1), 15–46. doi:10.4152/pea.200801015

Brillas, E., and Martínez-Huitle, C. A. (2011). *Synthetic diamond films: Preparation, electrochemistry, characterization, and applications*. New York, United States: Wiley.

Brillas, E., Sires, I., Arias, C., Cabot, P. L., Centellas, F., Rodriguez, R. M., et al. (2005). Mineralization of paracetamol in aqueous medium by anodic oxidation with a boron-doped diamond electrode. *Chemosphere* 58 (4), 399–406. doi:10.1016/j.chemosphere.2004.09.028

Brito, C. N., Ferreira, M. B., de, O., Marcionilio, S. M. L., de Moura Santos, E. C. M., Léon, J. J. L., et al. (2018). Electrochemical oxidation of acid violet 7 dye by using Si/BDD and Nb/BDD electrodes. *J. Electrochem. Soc.* 165 (5), E250–E255. doi:10.1149/2.1111805jes

Bushuev, E. V., Yurov, V. Y., Bolshakov, A. P., Ralchenko, V. G., Khomich, A. A., Antonova, I. A., et al. (2017). Express *in situ* measurement of epitaxial CVD diamond film growth kinetics. *Diam. Relat. Mater.* 72, 61–70. doi:10.1016/j.diamond.2016.12.021

Cano, A., Barrera, C., Cotillas, S., Llanos, J., Cañizares, P., and Rodrigo, M. A. (2016). Use of DiaCell modules for the electro-disinfection of secondary-treated wastewater with diamond anodes. *Chem. Eng. J.* 306, 433–440. doi:10.1016/j.cej.2016.07.090

Cano, A., Cañizares, P., Barrera, C., Sáez, C., and Rodrigo, M. A. (2011). Use of low current densities in electrolyses with conductive-diamond electrochemical — oxidation to disinfect treated wastewaters for reuse. *Electrochem. Commun.* 13 (11), 1268–1270. doi:10.1016/j.elecom.2011.08.027

Chang, M., Gao, C., and Jiang, J. (2009). Electrochemical oxidation of organic compounds using boron-doped diamond electrode. *J. Electrochem. Soc.* 156 (2), E50–E54. doi:10.1149/1.3042220

Chaplin, B. P. (2014). Critical review of electrochemical advanced oxidation processes for water treatment applications. *Environ. Sci. Process Impacts* 16 (6), 1182–1203. doi:10.1039/c3em00679d

Chaplin, B. P., Wyle, I., Zeng, H., Carlisle, J. A., and Farrell, J. (2011). Characterization of the performance and failure mechanisms of boron-doped ultrananocrystalline diamond electrodes. *J. Appl. Electrochem.* 41 (11), 1329–1340. doi:10.1007/s10800-011-0351-7

Chaudhuri, S., Hall, S. J., Klein, B. P., Walker, M., Logsdail, A. J., Macpherson, J. V., et al. (2022). Coexistence of carbonyl and ether groups on oxygen-terminated (110)-oriented diamond surfaces. *Commun. Mater.* 3 (1), 6. doi:10.1038/s43246-022-00228-4

Chen, G. (2004). Electrochemical technologies in wastewater treatment. *Sep. Purif. Technol.* 38 (1), 11–41. doi:10.1016/j.seppur.2003.10.006

Chen, P., Mu, Y., Chen, Y., Tian, L., Jiang, X. H., Zou, J. P., et al. (2022). Shifts of surface-bound *OH to homogeneous *OH in BDD electrochemical system via UV irradiation for enhanced degradation of hydrophilic aromatic compounds. *Chemosphere* 291, 132817. doi:10.1016/j.chemosphere.2021.132817

Chen, T.-S., Chen, P.-H., and Huang, K.-L. (2014). Electrochemical degradation of N,N-diethyl-m-toluamide on a boron-doped diamond electrode. *J. Taiwan Inst. Chem. Eng.* 45 (5), 2615–2621. doi:10.1016/j.jtice.2014.06.020

Chen, X., and Chen, G. (2004). Proper hot filament CVD conditions for fabrication of Ti-boron doped diamond electrodes. *J. Electrochem. Soc.* 151 (4), B214–B219. doi:10.1149/1.1651529

Chen, X., Gao, F., and Chen, G. (2005). Comparison of Ti/BDD and Ti/SnO2? Sb2O5 electrodes for pollutant oxidation. *J. Appl. Electrochem.* 35 (2), 185–191. doi:10.1007/s10800-004-6068-0

Choi, Y. S., Lee, Y. K., Kim, J. Y., Kim, K. M., and Lee, Y. K. (2017). Influence of manufacturing conditions for the life time of the boron-doped diamond electrode in wastewater treatment. *Korean J. Mater. Res.* 27 (3), 137–143. doi:10.3740/Mrsk.2017.27.3.137

Cifre, J., Puigdollers, J., Polo, M. C., and Esteve, J. (1994). Trimethylboron doping of CVD diamond thin films. *Diam. Relat. Mater.* 3 (4-6), 628–631. doi:10.1016/0925-9635(94)90238-0

Clematis, D., Cerisola, G., and Panizza, M. (2017). Electrochemical oxidation of a synthetic dye using a BDD anode with a solid polymer electrolyte. *Electrochem. Commun.* 75, 21–24. doi:10.1016/j.elecom.2016.12.008

Clematis, D., and Panizza, M. (2021a). Application of boron-doped diamond electrodes for electrochemical oxidation of real wastewaters. *Curr. Opin. Electrochem.* 30, 100844. ARTN 100844. doi:10.1016/j.coelec.2021.100844

Clematis, D., and Panizza, M. (2021b). Electrochemical oxidation of organic pollutants in low conductive solutions. *Curr. Opin. Electrochem.* 26, 100665. doi:10.1016/j.coelec.2020.100665

Cobb, S. J., Ayres, Z. J., and Macpherson, J. V. (2018). "Boron doped diamond: A designer electrode material for the twenty-first century," in *Annual review of analytical chemistry* (San Mateo, California: Annual Reviews).

Comninellis, C., Kapalka, A., Malato, S., Parsons, S. A., Poulios, I., and Mantzavinos, D. (2008). Advanced oxidation processes for water treatment: Advances and trends for R&D. *J. Chem. Technol. Biotechnol.* 83 (6), 769–776. doi:10.1002/jctb.1873

Comninellis, C., and Pulgarin, C. (1991). Anodic oxidation of phenol for waste water treatment. *J. Appl. Electrochem.* 21 (8), 703–708. doi:10.1007/bf01034049

Cornejo, O. M., Murrieta, M. F., Castañeda, L. F., and Nava, J. L. (2020). Characterization of the reaction environment in flow reactors fitted with BDD electrodes for use in electrochemical advanced oxidation processes: A critical review. *Electrochimica Acta* 331, 135373. doi:10.1016/j.electacta.2019.135373

Cornejo, O. M., Murrieta, M. F., Castañeda, L. F., and Nava, J. L. (2021). Electrochemical reactors equipped with BDD electrodes: Geometrical aspects and applications in water treatment. *Curr. Opin. Solid State Mater. Sci.* 25 (4), 100935. doi:10.1016/j.cossms.2021.100935

Cotillas, S., de Vidales, M. J., Llanos, J., Saez, C., Canizares, P., and Rodrigo, M. A. (2016). Electrolytic and electro-irradiated processes with diamond anodes for the oxidation of persistent pollutants and disinfection of urban treated wastewater. *J. Hazard Mater* 319, 93–101. doi:10.1016/j.jhazmat.2016.01.050

Crispim, A. C., da Silva Mendonça de Paiva, S., de Araújo, D. M., Souza, F. L., and Dos Santos, E. V. (2022). Ultrasound and UV technologies for wastewater treatment using boron-doped diamond anodes. *Curr. Opin. Electrochem.* 33, 100935. doi:10.1016/j.coelec.2021.100935

da Silva, S. W., Navarro, E. M. O., Rodrigues, M. A. S., Bernardes, A. M., and Perez-Herranz, V. (2018). The role of the anode material and water matrix in the electrochemical oxidation of norfloxacin. *Chemosphere* 210, 615–623. doi:10.1016/j.chemosphere.2018.07.057

Daskalaki, V. M., Fulgione, I., Frontistis, Z., Rizzo, L., and Mantzavinos, D. (2013). Solar light-induced photoelectrocatalytic degradation of bisphenol-A on TiO2/ITO film anode and BDD cathode. *Catal. Today* 209, 74–78. doi:10.1016/j.cattod.2012.07.026

De Luna, Y., and Bensalah, N. (2022). Review on the electrochemical oxidation of endocrine-disrupting chemicals using BDD anodes. *Curr. Opin. Electrochem.* 32, 100900. doi:10.1016/j.coelec.2021.100900

de Queiroz, J. L. A., da Silva, A. R. L., de Moura, D. C., da Silva, D. R., and Martínez-Huitle, C. A. (2017). Electrochemical study of carboxylic acids with Nb-supported boron doped diamond anode. Part 1: Potentiodynamic measurements and bulk oxidations. *J. Electroanal. Chem.* 794, 204–211. doi:10.1016/j.jelechem.2017.04.006

de Souza, R. B. A., and Ruotolo, L. A. M. (2013). Phenol electrooxidation in different supporting electrolytes using boron-doped diamond anodes. *Int. J. Electrochem. Sci.* 8 (1), 643–657.

Denisenko, A., Pietzka, C., Romanyuk, A., El-Hajj, H., and Kohn, E. (2008). The electronic surface barrier of boron-doped diamond by anodic oxidation. *J. Appl. Phys.* 103 (1), 014904. doi:10.1063/1.2827481

Dettlaff, A., Sobaszek, M., Klimczuk, T., and Bogdanowicz, R. (2021). Enhanced electrochemical kinetics of highly-oriented (111)-textured boron-doped diamond electrodes induced by deuterium plasma chemistry. *Carbon* 174, 594–604. doi:10.1016/j.carbon.2020.11.096

Donthu, N., Kumar, S., Mukherjee, D., Pandey, N., and Lim, W. M. (2021). How to conduct a bibliometric analysis: An overview and guidelines. *J. Bus. Res.* 133, 285–296. doi:10.1016/j.jbusres.2021.04.070

Durán, F. E., de Araújo, D. M., do Nascimento Brito, C., Santos, E. V., Ganiyu, S. O., and Martínez-Huitle, C. A. (2018). Electrochemical technology for the treatment of real washing machine effluent at pre-pilot plant scale by using active and non-active anodes. *J. Electroanal. Chem.* 818, 216–222. doi:10.1016/j.jelechem.2018.04.029

Dychalska, A., Popielarski, P., Franków, W., Fabisiak, K., Paprocki, K., and Szybowicz, M. (2015). Study of CVD diamond layers with amorphous carbon admixture by Raman scattering spectroscopy. *Mater. Pol.* 33 (4), 799–805. doi:10.1515/msp-2015-0067

Einaga, Y. (2018). Development of electrochemical applications of boron-doped diamond electrodes. *Bull. Chem. Soc. Jpn.* 91 (12), 1752–1762. doi:10.1246/bcsj.20180268

Einaga, Y., Foord, J. S., and Swain, G. M. (2014). Diamond electrodes: Diversity and maturity. *MRS Bull.* 39 (6), 525–532. doi:10.1557/mrs.2014.94

Enache, T. A., Chiorcea-Paquim, A.-M., Fatibello-Filho, O., and Oliveira-Brett, A. M. (2009). Hydroxyl radicals electrochemically generated *in situ* on a boron-doped diamond electrode. *Electrochem. Commun.* 11 (7), 1342–1345. doi:10.1016/j.elecom.2009.04.017

Espinoza, L. C., Aranda, M., Contreras, D., Henríquez, A., and Salazar, R. (2019). Effect of the sp3/sp2 ratio in boron-doped diamond electrodes on the degradation pathway of aniline by anodic oxidation. *ChemElectroChem* 6 (18), 4801–4810. doi:10.1002/celc.201901218

Espinoza-Montero, P. J., Vasquez-Medrano, R., Ibanez, J. G., and Frontana-Uribe, B. A. (2013). Efficient anodic degradation of phenol paired to improved cathodic production of H2O2at BDD electrodes. *J. Electrochem. Soc.* 160 (7), G3171–G3177. doi:10.1149/2.027307jes

Fabianska, A., Bialk-Bielinska, A., Stepnowski, P., Stolte, S., and Siedlecka, E. M. (2014). Electrochemical degradation of sulfonamides at BDD electrode: Kinetics, reaction pathway and eco-toxicity evaluation. *J. Hazard Mater* 280, 579–587. doi:10.1016/j.jhazmat.2014.08.050

Ferrari, A. C., and Robertson, J. (2004). Raman spectroscopy of amorphous, nanostructured, diamond-like carbon, and nanodiamond. *Philos. Trans. A Math. Phys. Eng. Sci.* 362 (1824), 2477–2512. doi:10.1098/rsta.2004.1452

Flox, C., Garrido, J. A., Rodríguez, R. M., Cabot, P.-L., Centellas, F., Arias, C., et al. (2007). Mineralization of herbicide mecoprop by photoelectro-Fenton with UVA and solar light. *Catal. Today* 129 (1-2), 29–36. doi:10.1016/j.cattod.2007.06.049

Freitas, J. M., Oliveira, T. D. C., Munoz, R. A. A., and Richter, E. M. (2019). Boron doped diamond electrodes in flow-based systems. *Front. Chem.* 7 (APR), 190. doi:10.3389/fchem.2019.00190

Fryda, M., Herrmann, D., Schafer, L., Klages, C. P., Perret, A., Haenni, W., et al. (1999). Properties of diamond electrodes for wastewater treatment. *New Diam. Front. Carbon Technol.* 9 (3), 229–240.

Ganiyu, S. O., and Martínez-Huitle, C. A. (2019). Nature, mechanisms and reactivity of electrogenerated reactive species at thin-film boron-doped diamond (BDD) electrodes during electrochemical wastewater treatment. *ChemElectroChem* 6 (9), 2379–2392. doi:10.1002/celc.201900159

Gerger, I., and Haubner, R. (2008). The behaviour of Ti-substrates during deposition of boron doped diamond. *Int. J. Refract. Metals Hard Mater.* 26 (5), 438–443. doi:10.1016/j.ijrmhm.2007.10.002

Gheeraert, E., Gonon, P., Deneuville, A., Abello, L., and Lucazeau, G. (1993). Effect of boron incorporation on the "quality" of MPCVD diamond films. *Diam. Relat. Mater.* 2 (5-7), 742–745. doi:10.1016/0925-9635(93)90215-n

Gomez-Ruiz, B., Diban, N., and Urtiaga, A. (2019). Comparison of microcrystalline and ultrananocrystalline boron doped diamond anodes: Influence on perfluorooctanoic acid electrolysis. *Sep. Purif. Technol.* 208, 169–177. doi:10.1016/j.seppur.2018.03.044

Gracio, J. J., Fan, Q. H., and Madaleno, J. C. (2010). Diamond growth by chemical vapour deposition. *J. Phys. D Appl. Phys.* 43 (37), 374017. doi:10.1088/0022-3727/43/37/374017

Griesser, M., Stingeder, G., Grasserbauer, M., Baumann, H., Link, F., Wurzinger, P., et al. (1994). Characterization of tantalum impurities in hot-filament diamond layers. *Diam. Relat. Mater.* 3 (4-6), 638–644. doi:10.1016/0925-9635(94)90240-2

Groenen Serrano, K., Savall, A., Latapie, L., Racaud, C., Rondet, P., and Bertrand, N. (2015). Performance of Ti/Pt and Nb/BDD anodes for dechlorination of nitric acid and regeneration of silver(II) in a tubular reactor for the treatment of solid wastes in nuclear industry. *J. Appl. Electrochem.* 45 (7), 779–786. doi:10.1007/s10800-015-0830-3

Guedes, V. L. S., and Borschiver, S. I. (2005). "Bibliometria: uma ferramenta estatística para a gestão da informação e do conhecimento em sistemas de informação, de comunicação e de avaliação científica e tecnológica," in *Encontro Nacional de Ciência da Informação*, 1–18. Salvador, Brazil: VI CINFORM Encontro Nacional de Ciência da Informação.

Guimaraes, G. A. A., Lacerda, J. N., Xing, Y., Ponzio, E. A., Pacheco, W. F., Semaan, F. S., et al. (2020). Development and application of electrochemical sensor of boron-doped diamond (BDD) modified by drop casting with tin hexacyanoferrate. *J. Solid State Electrochem.* 24 (8), 1769–1779. doi:10.1007/s10008-020-04558-6

Guo, L., and Chen, G. (2007). Long-term stable Ti/BDD electrode fabricated with HFCVD method using two-stage substrate temperature. *J. Electrochem. Soc.* 154 (12), D657–D661. doi:10.1149/1.2790798

Haenni, W., Rychen, P., Fryda, M., and Comninellis, C. (2004). "Chapter 5 Industrial applications of diamond electrodes," in *Thin-film diamond II*. Editors C. E. Nebel and J. Ristein (Amsterdam, Netherlands: Elsevier), 149–196.

Hangarter, C. M., O'Grady, W. E., Stoner, B. R., and Natishan, P. M. (2015). Electrochemical oxidation of phenol using boron-doped diamond electrodes. *ECS Trans.* 64 (46), 1–9. doi:10.1149/06446.0001ecst

He, Y., Huang, W., Chen, R., Zhang, W., and Lin, H. (2015). Improved electrochemical performance of boron-doped diamond electrode depending on the structure of titanium substrate. *J. Electroanal. Chem.* 758, 170–177. doi:10.1016/j.jelechem.2015.08.017

He, Y., Lin, H., Guo, Z., Zhang, W., Li, H., and Huang, W. (2019). Recent developments and advances in boron-doped diamond electrodes for electrochemical oxidation of organic pollutants. *Sep. Purif. Technol.* 212, 802–821. doi:10.1016/j.seppur.2018.11.056

He, Y., Wang, X., Huang, W., Chen, R., Lin, H., and Li, H. (2016). Application of porous boron-doped diamond electrode towards electrochemical mineralization of triphenylmethane dye. *J. Electroanal. Chem.* 775, 292–298. doi:10.1016/j.jelechem.2016.06.023

He, Y., Zhao, D., Lin, H., Huang, H., Li, H., and Guo, Z. (2022). Design of diamond anodes in electrochemical degradation of organic pollutants. *Curr. Opin. Electrochem.* 32, 100878. doi:10.1016/j.coelec.2021.100878

Huang, K.-L., Chao, P.-J., Kuo, Y.-M., Chi, K.-Y., Cheng, H. M., Wu, R.-Z., et al. (2021). Response surface methodology-based fabrication of boron-doped diamond electrodes for electrochemical degradation of guaifenesin in aqueous solutions. *J. Taiwan Inst. Chem. Eng.* 123, 124–133. doi:10.1016/j.jtice.2021.05.035

Huang, Y. H., Chen, C. C., Huang, G. H., and Chou, S. S. (2001). Comparison of a novel electro-Fenton method with Fenton's reagent in treating a highly contaminated wastewater. *Water Sci. Technol.* 43 (2), 17–24. doi:10.2166/wst.2001.0068

Hurwitz, G., Hoek, E. M. V., Liu, K., Fan, L., and Roddick, F. A. (2014). Photo-assisted electrochemical treatment of municipal wastewater reverse osmosis concentrate. *Chem. Eng. J.* 249, 180–188. doi:10.1016/j.cej.2014.03.084

Hutton, L. A., Iacobini, J. G., Bitziou, E., Channon, R. B., Newton, M. E., and Macpherson, J. V. (2013). Examination of the factors affecting the electrochemical performance of oxygen-terminated polycrystalline boron-doped diamond electrodes. *Anal. Chem.* 85 (15), 7230–7240. doi:10.1021/ac401042t

Iniesta, J. (2001). Electrochemical oxidation of phenol at boron-doped diamond electrode. *Electrochimica Acta* 46 (23), 3573–3578. doi:10.1016/s0013-4686(01)00630-2

Isshiki, H., Yoshida, M., Tobita, R., Shigeeda, T., Kinoshita, M., Matsushima, K., et al. (2012). Enhancement of diamond nucleation by atomic silicon microaddition. *Jpn. J. Appl. Phys.* 51 (9), 090108. doi:10.1143/jjap.51.090108

Jagannadham, K., Lance, M. J., and Butler, J. E. (2010). Laser annealing of neutron irradiated boron-10 isotope doped diamond. *J. Mater. Sci.* 46 (8), 2518–2528. doi:10.1007/s10853-010-5102-3

Jia, F.-c., Bai, Y.-z., Qu, F., Sun, J., Zhao, J.-j., and Jiang, X. (2010). The influence of gas pressure and bias current on the crystallinity of highly boron-doped diamond films. *New Carbon Mater.* 25 (5), 357–362. doi:10.1016/s1872-5805(09)60039-1

Jian, Z., Heide, M., Yang, N., Engelhard, C., and Jiang, X. (2021). Diamond fibers for efficient electrocatalytic degradation of environmental pollutants. *Carbon* 175, 36–42. doi:10.1016/j.carbon.2020.12.066

Jiang, J., Chang, M., and Pan, P. (2008). Simultaneous hydrogen production and electrochemical oxidation of organics using boron-doped diamond electrodes. *Environ. Sci. Technol.* 42 (8), 3059–3063. doi:10.1021/es702466k

Kapałka, A., Lanova, B., Baltruschat, H., Fóti, G. r., and Comninellis, C. (2009). A DEMS study of methanol and formic acid oxidation on boron-doped diamond electrode. *J. Electrochem. Soc.* 156 (11), E149–E153. doi:10.1149/1.3207009

Karim, A. V., Nidheesh, P. V., and Oturan, M. A. (2021). Boron-doped diamond electrodes for the mineralization of organic pollutants in the real wastewater. *Curr. Opin. Electrochem.* 30, 100855. doi:10.1016/j.coelec.2021.100855

Kondo, T., Ito, H., Kusakabe, K., Ohkawa, K., Einaga, Y., Fujishima, A., et al. (2007). Plasma etching treatment for surface modification of boron-doped diamond electrodes. *Electrochimica Acta* 52 (11), 3841–3848. doi:10.1016/j.electacta.2006.11.001

Kornienko, G. V., Chaenko, N. V., Maksimov, N. G., Kornienko, V. L., and Varnin, V. P. (2011). Electrochemical oxidation of phenol on boron-doped diamond electrode. *Russ. J. Electrochem.* 47 (2), 225–229. doi:10.1134/s102319351102011x

Kowalska, M., Paprocki, K., Szybowicz, M., Wrzyszczyński, A., Łoś, S., and Fabisiak, K. (2020). Electrochemical sensitivity of undoped CVD diamond films as function of their crystalline quality. *J. Electroanal. Chem.* 859, 113811. doi:10.1016/j.jelechem.2019.113811

Kuchtová, G., Chýlková, J., Váňa, J., Vojs, M., and Dušek, L. (2020). Electro-oxidative decolorization and treatment of model wastewater containing Acid Blue 80 on boron doped diamond and platinum anodes. *J. Electroanal. Chem.* 863, 114036. doi:10.1016/j.jelechem.2020.114036

Kwon, J.-I., You, M., Kim, S., and Keun, S. P. (2019). Performance of BDD electrodes prepared on various substrates for wastewater treatment. *J. Korean Inst. Surf. Eng.* 52 (2), 53–57. doi:10.5695/JKISE.2019.52.2.53

Lacasa, E., Tsolaki, E., Sbokou, Z., Rodrigo, M. A., Mantzavinos, D., and Diamadopoulos, E. (2013). Electrochemical disinfection of simulated ballast water on conductive diamond electrodes. *Chem. Eng. J.* 223, 516–523. doi:10.1016/j.cej.2013.03.003

Lagrange, J. P., Deneuville, A., and Gheeraert, E. (1998). Activation energy in low compensated homoepitaxial boron-doped diamond films. *Diam. Relat. Mater.* 7 (9), 1390–1393. doi:10.1016/s0925-9635(98)00225-8

Larsson, K. (2020). "Simulation of diamond surface chemistry: Reactivity and properties," in *Some aspects of diamonds in scientific research and high technology*. Editor E. Lipatov (London: IntechOpen).

Lee, C.-H., Lee, E.-S., Lim, Y.-K., Park, K.-H., Park, H.-D., and Lim, D.-S. (2017). Enhanced electrochemical oxidation of phenol by boron-doped diamond nanowire electrode. *RSC Adv.* 7 (11), 6229–6235. doi:10.1039/c6ra26287b

Lee, K. H., Seong, W. K., and Ruoff, R. S. (2022). CVD diamond growth: Replacing the hot metallic filament with a hot graphite plate. *Carbon* 187, 396–403. doi:10.1016/j.carbon.2021.11.032

Lévy-Clément, C., Ndao, N. A., Katty, A., Bernard, M., Deneuville, A., Comninellis, C., et al. (2003). Boron doped diamond electrodes for nitrate elimination in concentrated wastewater. *Diam. Relat. Mater.* 12 (3-7), 606–612. doi:10.1016/s0925-9635(02)00368-0

Li, H., Yu, Q., Yang, B., Li, Z., and Lei, L. (2015). Electro-catalytic oxidation of artificial human urine by using BDD and IrO2 electrodes. *J. Electroanal. Chem.* 738, 14–19. doi:10.1016/j.jelechem.2014.11.018

Li, H., Yu, Q., Yang, B., Li, Z., and Lei, L. (2014). Electrochemical treatment of artificial humidity condensate by large-scale boron doped diamond electrode. *Sep. Purif. Technol.* 138, 13–20. doi:10.1016/j.seppur.2014.10.004

Li, W., Liu, G., Miao, D., Li, Z., Chen, Y., Gao, X., et al. (2020). Electrochemical oxidation of Reactive Blue 19 on boron-doped diamond anode with different supporting electrolyte. *J. Environ. Chem. Eng.* 8 (4), 103997. doi:10.1016/j.jece.2020.103997

Li, X., Li, H., Li, M., Li, C., Sun, D., Lei, Y., et al. (2018). Preparation of a porous boron-doped diamond/Ta electrode for the electrocatalytic degradation of organic pollutants. *Carbon* 129, 543–551. doi:10.1016/j.carbon.2017.12.052

Lim, P. Y., Lin, F. Y., Shih, H. C., Ralchenko, V. G., Varnin, V. P., Pleskov, Y. V., et al. (2008). Improved stability of titanium based boron-doped chemical vapor deposited diamond thin-film electrode by modifying titanium substrate surface. *Thin Solid Films* 516 (18), 6125–6132. doi:10.1016/j.tsf.2007.11.016

Liu, F. B., Wang, J. D., Liu, B., Li, X. M., and Chen, D. R. (2007). Effect of electronic structures on electrochemical behaviors of surface-terminated boron-doped diamond film electrodes. *Diam. Relat. Mater.* 16 (3), 454–460. doi:10.1016/j.diamond.2006.08.016

Liu, Z., Li, H., Li, M., Li, C., Qian, L., Su, L., et al. (2018). Preparation of polycrystalline BDD/Ta electrodes for electrochemical oxidation of organic matter. *Electrochimica Acta* 290, 109–117. doi:10.1016/j.electacta.2018.09.058

Lourencao, B. C., Brocenschi, R. F., Medeiros, R. A., Fatibello-Filho, O., and Rocha-Filho, R. C. (2020). Analytical applications of electrochemically pretreated boron-doped diamond electrodes. *ChemElectroChem* 7 (6), 1291–1311. doi:10.1002/celc.202000050

Lu, X.-R., Ding, M.-H., Zhang, C., and Tang, W.-Z. (2019a). Comparative study on stability of boron doped diamond coated titanium and niobium electrodes. *Diam. Relat. Mater.* 93, 26–33. doi:10.1016/j.diamond.2019.01.010

Lu, X. R., Ding, M. H., Zhang, C., and Tang, W. Z. (2018). Investigation on microstructure evolution and failure mechanism of boron doped diamond coated titanium electrode during accelerated life test. *Thin Solid Films* 660, 306–313. doi:10.1016/j.tsf.2018.06.039

Lu, X. R., Ding, M. H., Zhang, L., Yang, Z. L., Lu, Y., and Tang, W. Z. (2019b). Optimizing the microstructure and corrosion resistance of BDD coating to improve the service life of Ti/BDD coated electrode. *Materials* 12 (19), 3188. doi:10.3390/ma12193188

Lu, Y.-G., Turner, S., Verbeeck, J., Janssens, S. D., Wagner, P., Haenen, K., et al. (2012). Direct visualization of boron dopant distribution and coordination in individual chemical vapor deposition nanocrystalline B-doped diamond grains. *Appl. Phys. Lett.* 101 (4), 041907. doi:10.1063/1.4738885

Luong, J. H., Male, K. B., and Glennon, J. D. (2009). Boron-doped diamond electrode: Synthesis, characterization, functionalization and analytical applications. *Analyst* 134 (10), 1965–1979. doi:10.1039/b910206j

Ma, P., Ma, H., Sabatino, S., Galia, A., and Scialdone, O. (2018). Electrochemical treatment of real wastewater. Part 1: Effluents with low conductivity. *Chem. Eng. J.* 336, 133–140. doi:10.1016/j.cej.2017.11.046

Machini, W. B. S., Enache, T. A., Jorge, S. M. A., and Oliveira-Brett, A. M. (2016). Isotretinoin oxidation and electroanalysis in a pharmaceutical drug using a boron-doped diamond electrode. *Electroanalysis* 28 (11), 2709–2715. doi:10.1002/elan.201600206

Mackuľak, T., Medvecká, E., Vojs Staňová, A., Brandeburová, P., Grabic, R., Golovko, O., et al. (2020). Boron doped diamond electrode – the elimination of psychoactive drugs and resistant bacteria from wastewater. *Vacuum* 171, 108957. doi:10.1016/j.vacuum.2019.108957

Macpherson, J. V. (2015). A practical guide to using boron doped diamond in electrochemical research. *Phys. Chem. Chem. Phys.* 17 (5), 2935–2949. doi:10.1039/c4cp04022h

Maldonado, V. Y., Becker, M. F., Nickelsen, M. G., and Witt, S. E. (2021). Laboratory and semi-pilot scale study on the electrochemical treatment of perfluoroalkyl acids from ion exchange still bottoms. *Water* 13 (20), 2873. doi:10.3390/w13202873

Martin, H. B., Argoitia, A., Landau, U., Anderson, A. B., and Angus, J. C. (2019). Hydrogen and oxygen evolution on boron-doped diamond electrodes. *J. Electrochem. Soc.* 143 (6), L133–L136. doi:10.1149/1.1836901

May, P. W., Ludlow, W. J., Hannaway, M., Smith, J. A., Rosser, K. N., and Heard, P. J. (2011). Boron doping of microcrystalline and nanocrystalline diamond films: Where is the boron going? *MRS Proc.* 1039. doi:10.1557/proc-1039-p17-03

McBeath, S. T., Wilkinson, D. P., and Graham, N. J. D. (2019). Application of boron-doped diamond electrodes for the anodic oxidation of pesticide micropollutants in a water treatment process: A critical review. *Environ. Sci. Water Res. Technol.* 5 (12), 2090–2107. doi:10.1039/c9ew00589g

McLaughlin, M. H. S., Corcoran, E., Pakpour-Tabrizi, A. C., de Faria, D. C., and Jackman, R. B. (2020). Influence of temperature on the electrochemical window of boron doped diamond: A comparison of commercially available electrodes. *Sci. Rep.* 10 (1), 15707. doi:10.1038/s41598-020-72910-x

McNamara, K. M., Gleason, K. K., Vestyck, D. J., and Butler, J. E. (1992). Evaluation of diamond films by nuclear magnetic resonance and Raman spectroscopy. *Diam. Relat. Mater.* 1 (12), 1145–1155. doi:10.1016/0925-9635(92)90088-6

Medeiros de Araújo, D., Cañizares, P., Martínez-Huitle, C. A., and Rodrigo, M. A. (2014). Electrochemical conversion/combustion of a model organic pollutant on BDD anode: Role of sp 3/sp 2 ratio. *Electrochem. Commun.* 47, 37–40. doi:10.1016/j.elecom.2014.07.017

Mehedi, H. A., Achard, J., Rats, D., Brinza, O., Tallaire, A., Mille, V., et al. (2014). Low temperature and large area deposition of nanocrystalline diamond films with distributed antenna array microwave-plasma reactor. *Diam. Relat. Mater.* 47, 58–65. doi:10.1016/j.diamond.2014.05.004

Mehta Menon, P., Edwards, A., Feigerle, C. S., Shaw, R. W., Coffey, D. W., Heatherly, L., et al. (1999). Filament metal contamination and Raman spectra of hot filament chemical vapor deposited diamond films. *Diam. Relat. Mater.* 8 (1), 101–109. doi:10.1016/s0925-9635(98)00444-0

Miao, D., Li, Z., Chen, Y., Liu, G., Deng, Z., Yu, Y., et al. (2022). Preparation of macro-porous 3D boron-doped diamond electrode with surface micro structure regulation to enhance electrochemical degradation performance. *Chem. Eng. J.* 429, 132366. doi:10.1016/j.cej.2021.132366

Miao, D., Liu, T., Yu, Y., Li, S., Liu, G., Chen, Y., et al. (2020). Study on degradation performance and stability of high temperature etching boron-doped diamond electrode. *Appl. Surf. Sci.* 514, 146091. doi:10.1016/j.apsusc.2020.146091

Migliorini, F. L., Steter, J. R., Rocha, R. S., Lanza, M. R. V., Baldan, M. R., and Ferreira, N. G. (2016). Efficiency study and mechanistic aspects in the Brilliant Green dye degradation using BDD/Ti electrodes. *Diam. Relat. Mater.* 65, 5–12. doi:10.1016/j.diamond.2015.12.013

Mitadera, M., Spataru, N., and Fujishima, A. (2004). Electrochemical oxidation of aniline at boron-doped diamond electrodes. *J. Appl. Electrochem.* 34 (3), 249–254. doi:10.1023/b:Jach.0000015623.63462.60

Mitra, P., Chattopadhyay, K. K., Chaudhuri, S., and Pal, A. K. (1994). Electrical properties of boron-doped diamond films prepared by dc plasma decomposition of CO2 + H2. *Mater. Lett.* 21 (1), 95–99. doi:10.1016/0167-577x(94)90130-9

Moelle, C., Klose, S., Szücs, F., Fecht, H. J., Johnston, C., Chalker, P. R., et al. (1997). Measurement and calculation of the thermal expansion coefficient of diamond. *Diam. Relat. Mater.* 6 (5-7), 839–842. doi:10.1016/s0925-9635(96)00674-7

Monteil, H., Pechaud, Y., Oturan, N., Trellu, C., and Oturan, M. A. (2021). Pilot scale continuous reactor for water treatment by electrochemical advanced oxidation processes: Development of a new hydrodynamic/reactive combined model. *Chem. Eng. J.* 404, 127048. doi:10.1016/j.cej.2020.127048

Moreira, F. C., Boaventura, R. A. R., Brillas, E., and Vilar, V. J. P. (2017). Electrochemical advanced oxidation processes: A review on their application to synthetic and real wastewaters. *Appl. Catal. B Environ.* 202, 217–261. doi:10.1016/j.apcatb.2016.08.037

Mousavi, M. P. S., Dittmer, A. J., Wilson, B. E., Hu, J., Stein, A., and Bühlmann, P. (2015). Unbiased quantification of the electrochemical stability limits of electrolytes and ionic liquids. *J. Electrochem. Soc.* 162 (12), A2250–A2258. doi:10.1149/2.0271512jes

Mousset, E. (2022). Interest of micro-reactors for the implementation of advanced electrocatalytic oxidation with boron-doped diamond anode for wastewater treatment. *Curr. Opin. Electrochem.* 32, 100897. doi:10.1016/j.coelec.2021.100897

Murugananthan, M., Latha, S. S., Bhaskar Raju, G., and Yoshihara, S. (2011). Role of electrolyte on anodic mineralization of atenolol at boron doped diamond and Pt electrodes. *Sep. Purif. Technol.* 79 (1), 56–62. doi:10.1016/j.seppur.2011.03.011

Murugananthan, M., Yoshihara, S., Rakuma, T., Uehara, N., and Shirakashi, T. (2007). Electrochemical degradation of 17β-estradiol (E2) at boron-doped diamond (Si/BDD) thin film electrode. *Electrochimica Acta* 52 (9), 3242–3249. doi:10.1016/j.electacta.2006.09.073

Naji, T., Dirany, A., Carabin, A., and Drogui, P. (2017). Large-scale disinfection of real swimming pool water by electro-oxidation. *Environ. Chem. Lett.* 16 (2), 545–551. doi:10.1007/s10311-017-0687-2

Neto, M. A., Pato, G., Bundaleski, N., Teodoro, O. M. N. D., Fernandes, A. J. S., Oliveira, F. J., et al. (2016). Surface modifications on as-grown boron doped CVD diamond films induced by the B2O3–ethanol–Ar system. *Diam. Relat. Mater.* 64, 89–96. doi:10.1016/j.diamond.2016.02.001

Neto, M. A., Silva, E. L., Ghumman, C. A., Teodoro, O. M., Fernandes, A. J. S., Oliveira, F. J., et al. (2012). Composition profiles and adhesion evaluation of conductive diamond coatings on dielectric ceramics. *Thin Solid Films* 520 (16), 5260–5266. doi:10.1016/j.tsf.2012.03.049

Nidheesh, P. V., Divyapriya, G., Oturan, N., Trellu, C., and Oturan, M. A. (2019). Environmental applications of boron-doped diamond electrodes: 1. Applications in water and wastewater treatment. *ChemElectroChem* 6 (8), 2124–2142. doi:10.1002/celc.201801876

Notsu, H., Fukazawa, T., Tatsuma, T., Tryk, D. A., and Fujishima, A. (2001). Hydroxyl groups on boron-doped diamond electrodes and their modification with a silane coupling agent. *Electrochem. Solid-State Lett.* 4 (3), H1–H3. doi:10.1149/1.1346556

Oliveira, T. M. B. F., Ribeiro, F. W. P., Morais, S., de Lima-Neto, P., and Correia, A. N. (2022). Removal and sensing of emerging pollutants released from (micro)plastic degradation: Strategies based on boron-doped diamond electrodes. *Curr. Opin. Electrochem.* 31, 100866. doi:10.1016/j.coelec.2021.100866

Olson, E. J., and Bühlmann, P. (2012). Unbiased assessment of electrochemical windows: Minimizing mass transfer effects on the evaluation of anodic and cathodic limits. *J. Electrochem. Soc.* 160 (2), A320–A323. doi:10.1149/2.068302jes

Oturan, M. A., Sirés, I., Oturan, N., Pérocheau, S., Laborde, J.-L., and Trévin, S. (2008). Sonoelectro-fenton process: A novel hybrid technique for the destruction of organic pollutants in water. *J. Electroanal. Chem.* 624 (1-2), 329–332. doi:10.1016/j.jelechem.2008.08.005

Pacheco, M. J., Morão, A., Lopes, A., Ciríaco, L., and Gonçalves, I. (2007). Degradation of phenols using boron-doped diamond electrodes: A method for quantifying the extent of combustion. *Electrochimica Acta* 53 (2), 629–636. doi:10.1016/j.electacta.2007.07.024

Panizza, M., and Cerisola, G. (2009). Direct and mediated anodic oxidation of organic pollutants. *Chem. Rev.* 109 (12), 6541–6569. doi:10.1021/cr9001319

Panizza, M., Michaud, P. A., Cerisola, G., and Comninellis, C. (2001). Anodic oxidation of 2-naphthol at boron-doped diamond electrodes. *J. Electroanal. Chem.* 507 (1-2), 206–214. doi:10.1016/s0022-0728(01)00398-9

Parikh, R. P., and Adomaitis, R. A. (2006). An overview of gallium nitride growth chemistry and its effect on reactor design: Application to a planetary radial-flow CVD system. *J. Cryst. Growth* 286 (2), 259–278. doi:10.1016/j.jcrysgro.2005.09.050

ParitoshSrolovitz, D. J., Battaile, C. C., Li, X., and Butler, J. E. (1999). Simulation of faceted film growth in two-dimensions: Microstructure, morphology and texture. *Acta Mater.* 47 (7), 2269–2281. doi:10.1016/s1359-6454(99)00086-5

Patel, A. N., Tan, S. Y., Miller, T. S., Macpherson, J. V., and Unwin, P. R. (2013). Comparison and reappraisal of carbon electrodes for the voltammetric detection of dopamine. *Anal. Chem.* 85 (24), 11755–11764. doi:10.1021/ac401969q

Patel, K., Hashimoto, K., and Fujishima, A. (1992). Application of boron-doped CVD-diamond film to photoelectrode. *Denki Kagaku oyobi Kogyo Butsuri Kagaku* 60 (7), 659–661. doi:10.5796/electrochemistry.60.659

Pelskov, Y. V., Sakharova, A. Y., Krotova, M. D., Bouilov, L. L., and Spitsyn, B. V. (1987). Photoelectrochemical properties of semiconductor diamond. *J. Electroanal. Chem. Interfacial Electrochem.* 228 (1-2), 19–27. doi:10.1016/0022-0728(87)80093-1

Pleskov, Y. (2011). "Electrochemistry of diamond," in *Synthetic diamond films*. Editors E. Brillas and C. A. Martínez-Huitle, 77–108. Hoboken, New Jersey, United States: John Wiley& Sons, Inc.

Prawer, S., and Nemanich, R. J. (2004). Raman spectroscopy of diamond and doped diamond. *Philos. Trans. A Math. Phys. Eng. Sci.* 362 (1824), 2537–2565. doi:10.1098/rsta.2004.1451

Pujol, A. A., León, I., Cárdenas, J., Sepúlveda-Guzmán, S., Manríquez, J., Sirés, I., et al. (2020). Degradation of phenols by heterogeneous electro-Fenton with a Fe3O4-chitosan composite and a boron-doped diamond anode. *Electrochimica Acta* 337, 135784. doi:10.1016/j.electacta.2020.135784

Railkar, T. A., Kang, W. P., Windischmann, H., Malshe, A. P., Naseem, H. A., Davidson, J. L., et al. (2000). A critical review of chemical vapor-deposited (CVD) diamond for electronic applications. *Crit. Rev. Solid State Mater. Sci.* 25 (3), 163–277. doi:10.1080/10408430008951119

Ramesham, R., and Rose, M. F. (1997). Electrochemical characterization of doped and undoped CVD diamond deposited by microwave plasma. *Diam. Relat. Mater.* 6 (1), 17–26. doi:10.1016/s0925-9635(96)00593-6

Read, T. L., and Macpherson, J. V. (2016). Assessment of boron doped diamond electrode quality and application to *in situ* modification of local pH by water electrolysis. *J. Vis. Exp.* 107, 53484. doi:10.3791/53484

Rivera, F. F., León, C. P. d., Walsh, F. C., and Nava, J. L. (2015). The reaction environment in a filter-press laboratory reactor: The FM01-LC flow cell. *Electrochimica Acta* 161, 436–452. doi:10.1016/j.electacta.2015.02.161

Roccamante, M., Salmerón, I., Ruiz, A., Oller, I., and Malato, S. (2020). New approaches to solar Advanced Oxidation Processes for elimination of priority substances based on electrooxidation and ozonation at pilot plant scale. *Catal. Today* 355, 844–850. doi:10.1016/j.cattod.2019.04.014

Rohatgi, A. (2019). *WebPlotDigitizer*. San Francisco, California, USA. Available: https://automeris.io/WebPlotDigitizer (Accessed 12 15, 2021).

Rubí-Juárez, H., Cotillas, S., Sáez, C., Cañizares, P., Barrera-Díaz, C., and Rodrigo, M. A. (2016). Use of conductive diamond photo-electrochemical oxidation for the removal of pesticide glyphosate. *Sep. Purif. Technol.* 167, 127–135. doi:10.1016/j.seppur.2016.04.048

Ryl, J., Burczyk, L., Bogdanowicz, R., Sobaszek, M., and Darowicki, K. (2016). Study on surface termination of boron-doped diamond electrodes under anodic polarization in H2SO4 by means of dynamic impedance technique. *Carbon* 96, 1093–1105. doi:10.1016/j.carbon.2015.10.064

Ryl, J., Burczyk, L., Zielinski, A., Ficek, M., Franczak, A., Bogdanowicz, R., et al. (2019). Heterogeneous oxidation of highly boron-doped diamond electrodes and its influence on the surface distribution of electrochemical activity. *Electrochimica Acta* 297, 1018–1027. doi:10.1016/j.electacta.2018.12.050

Salazar-Banda, G. R., Andrade, L. S., Nascente, P. A. P., Pizani, P. S., Rocha-Filho, R. C., and Avaca, L. A. (2006). On the changing electrochemical behaviour of boron-doped diamond surfaces with time after cathodic pre-treatments. *Electrochimica Acta* 51 (22), 4612–4619. doi:10.1016/j.electacta.2005.12.039

Salazar-Banda, G. R., de Carvalho, A. E., Andrade, L. S., Rocha-Filho, R. C., and Avaca, L. A. (2010). On the activation and physical degradation of boron-doped diamond surfaces brought on by cathodic pretreatments. *J. Appl. Electrochem.* 40 (10), 1817–1827. doi:10.1007/s10800-010-0139-1

Salgueiredo, E., Amaral, M., Neto, M. A., Fernandes, A. J. S., Oliveira, F. J., and Silva, R. F. (2011). HFCVD diamond deposition parameters optimized by a Taguchi Matrix. *Vacuum* 85 (6), 701–704. doi:10.1016/j.vacuum.2010.10.010

Salmeron, I., Oller, I., Plakas, K. V., and Malato, S. (2021). Carbon-based cathodes degradation during electro-Fenton treatment at pilot scale: Changes in H2O2 electrogeneration. *Chemosphere* 275, 129962. doi:10.1016/j.chemosphere.2021.129962

Salmerón, I., Plakas, K. V., Sirés, I., Oller, I., Maldonado, M. I., Karabelas, A. J., et al. (2019). Optimization of electrocatalytic H2O2 production at pilot plant scale for solar-assisted water treatment. *Appl. Catal. B Environ.* 242, 327–336. doi:10.1016/j.apcatb.2018.09.045

Schwander, M., and Partes, K. (2011). A review of diamond synthesis by CVD processes. *Diam. Relat. Mater.* 20 (9), 1287–1301. doi:10.1016/j.diamond.2011.08.005

Sein, H., Ahmed, W., Jackson, M., and Polini, R. (2006). *Growth of polycrystalline diamond on titanium nitride on silicon substrates using negative bias assisted CVD*. Materials Park: Asm International.

Sharma, D. K., Girao, A. V., Chapon, P., Neto, M. A., Oliveira, F. J., and Silva, R. F. (2022). Advances in RF glow discharge optical emission spectrometry characterization of intrinsic and boron-doped diamond coatings. *ACS Appl. Mater Interfaces* 14 (5), 7405–7416. doi:10.1021/acsami.1c20785

Shaw, J., Jones, A. N., Monk, P. M. S., and Rego, C. A. (2002). Electrochemical behaviour of graphite- and molybdenum electrodes modified with thin-film diamond. *Diam. Relat. Mater.* 11 (9), 1690–1696. doi:10.1016/s0925-9635(02)00139-5

Shroder, R. E., Nemanich, R. J., and Glass, J. T. (1990). Analysis of the composite structures in diamond thin films by Raman spectroscopy. *Phys. Rev. B Condens Matter* 41 (6), 3738–3745. doi:10.1103/physrevb.41.3738

Sires, I., Brillas, E., Oturan, M. A., Rodrigo, M. A., and Panizza, M. (2014). Electrochemical advanced oxidation processes: Today and tomorrow. A review. *Environ. Sci. Pollut. Res. Int.* 21 (14), 8336–8367. doi:10.1007/s11356-014-2783-1

Souza, F., Saéz, C., Lanza, M., Cañizares, P., and Rodrigo, M. A. (2016). Towards the scale-up of electrolysis with diamond anodes: Effect of stacking on the electrochemical oxidation of 2,4 D. *J. Chem. Technol. Biotechnol.* 91 (3), 742–747. doi:10.1002/jctb.4639

Spitsyn, B. V., Bouilov, L. L., and Derjaguin, B. V. (1981). Vapor growth of diamond on diamond and other surfaces. *J. Cryst. Growth* 52, 219–226. doi:10.1016/0022-0248(81)90197-4

Srikanth, V. V. S. S., and Jiang, X. (2011). "Synthesis of diamond films," in *Synthetic diamond films*, 21–55. Hoboken, New Jersey, United States: John Wiley& Sons, Inc.

Stanković, D. M., and Kalcher, K. (2016). Amperometric quantification of the pesticide ziram at boron doped diamond electrodes using flow injection analysis. *Sensors Actuators B Chem.* 233, 144–147. doi:10.1016/j.snb.2016.04.069

Štenclová, P., Vyskočil, V., Szabó, O., Ižák, T., Potocký, Š., and Kromka, A. (2019). Structured and graphitized boron doped diamond electrodes: Impact on electrochemical detection of Cd2+ and Pb2+ ions. *Vacuum* 170, 108953. doi:10.1016/j.vacuum.2019.108953

Sun, J., Lu, H., Lin, H., Huang, W., Li, H., Lu, J., et al. (2012). Boron doped diamond electrodes based on porous Ti substrates. *Mater. Lett.* 83, 112–114. doi:10.1016/j.matlet.2012.05.044

Swain, G. M., Anderson, A. B., and Angus, J. C. (2013). Applications of diamond thin films in electrochemistry. *MRS Bull.* 23 (9), 56–60. doi:10.1557/s0883769400029389

Swain, G. M., and Ramesham, R. (2002). The electrochemical activity of boron-doped polycrystalline diamond thin film electrodes. *Anal. Chem.* 65 (4), 345–351. doi:10.1021/ac00052a007

Swain, G. M. (2019). The susceptibility to surface corrosion in acidic fluoride media: A comparison of diamond, Hopg, and glassy carbon electrodes. *J. Electrochem. Soc.* 141 (12), 3382–3393. doi:10.1149/1.2059343

Swain, G. M. (1994). The use of CVD diamond thin films in electrochemical systems. *Adv. Mater.* 6 (5), 388–392. doi:10.1002/adma.19940060511

Tamor, M. A., and Everson, M. P. (2011). On the role of penetration twins in the morphological development of vapor-grown diamond films. *J. Mater. Res.* 9 (7), 1839–1849. doi:10.1557/jmr.1994.1839

Tang, C. J., Fernandes, A. J. S., Costa, F., and Pinto, J. L. (2011). Effect of microwave power and nitrogen addition on the formation of {100} faceted diamond from microcrystalline to nanocrystalline. *Vacuum* 85 (12), 1130–1134. doi:10.1016/j.vacuum.2011.01.024

Tawabini, B. S., Plakas, K. V., Fraim, M., Safi, E., Oyehan, T., and Karabelas, A. J. (2020). Assessing the efficiency of a pilot-scale GDE/BDD electrochemical system in removing phenol from high salinity waters. *Chemosphere* 239, 124714. doi:10.1016/j.chemosphere.2019.124714

Teraji, T., Yamamoto, T., Watanabe, K., Koide, Y., Isoya, J., Onoda, S., et al. (2015). Homoepitaxial diamond film growth: High purity, high crystalline quality, isotopic enrichment, and single color center formation. *Phys. status solidi (a)* 212 (11), 2365–2384. doi:10.1002/pssa.201532449

Trellu, C., Chakraborty, S., Nidheesh, P. V., and Oturan, M. A. (2019). Environmental applications of boron-doped diamond electrodes: 2. Soil remediation and sensing applications. *ChemElectroChem* 6 (8), 2143–2156. doi:10.1002/celc.201801877

Triana, Y., Tomisaki, M., and Einaga, Y. (2020). Oxidation reaction of dissolved hydrogen sulfide using boron doped diamond. *J. Electroanal. Chem.* 873, 114411. doi:10.1016/j.jelechem.2020.114411

Tryk, D. A., Tsunozaki, K., Rao, T. N., and Fujishima, A. (2001). Relationships between surface character and electrochemical processes on diamond electrodes: Dual roles of surface termination and near-surface hydrogen. *Diam. Relat. Mater.* 10 (9-10), 1804–1809. doi:10.1016/s0925-9635(01)00453-8

Ueda, A., Kato, D., Sekioka, N., Hirono, S., and Niwa, O. (2009). Local imaging of an electrochemical active/inactive region on a conductive carbon surface by using scanning electrochemical microscopy. *Anal. Sci.* 25 (5), 645–651. doi:10.2116/analsci.25.645

van der Drift, A. (1967). Evolutionary selection: A principle governing growth orientation in vapour deposited layers. *Philips Res. Rep.* 22, 267–288.

van Eck, N. J., and Waltman, L. (2010). Software survey: VOSviewer, a computer program for bibliometric mapping. *Scientometrics* 84 (2), 523–538. doi:10.1007/s11192-009-0146-3

Vanhove, E., de Sanoit, J., Arnault, J. C., Saada, S., Mer, C., Mailley, P., et al. (2007). Stability of H-terminated BDD electrodes: An insight into the influence of the surface preparation. *Phys. status solidi (a)* 204 (9), 2931–2939. doi:10.1002/pssa.200776340

Vernasqui, L. G., Sardinha, A. F., Oishi, S. S., and Ferreira, N. G. (2021). Nanoscale control of high-quality boron-doped ultrananodiamond on dioxide titanium nanotubes as a porous composite. *J. Mater. Res. Technol.* 12, 597–612. doi:10.1016/j.jmrt.2021.02.099

Vidales, M. J. M. d., Barba, S., Sáez, C., Cañizares, P., and Rodrigo, M. A. (2014). Coupling ultraviolet light and ultrasound irradiation with Conductive-Diamond Electrochemical Oxidation for the removal of progesterone. *Electrochimica Acta* 140, 20–26. doi:10.1016/j.electacta.2014.02.118

Vieira Dos Santos, E., Saez, C., Canizares, P., Martinez-Huitle, C. A., and Rodrigo, M. A. (2017). Treating soil-washing fluids polluted with oxyfluorfen by sono-electrolysis with diamond anodes. *Ultrason. Sonochem* 34, 115–122. doi:10.1016/j.ultsonch.2016.05.029

Vorlíček, V., Rosa, J., Vaněček, M., Nesládek, M., and Stals, L. M. (1997). Quantitative study of Raman scattering and defect optical absorption in CVD diamond films. *Diam. Relat. Mater.* 6 (5-7), 704–707. doi:10.1016/s0925-9635(96)00630-9

Wang, X. H., Ma, G. H. M., Zhu, W., Glass, J. T., Bergman, L., Turner, K. F., et al. (1992). Effects of boron doping on the surface morphology and structural imperfections of diamond films. *Diam. Relat. Mater.* 1 (7), 828–835. doi:10.1016/0925-9635(92)90109-2

Wang, Z., Liu, S., and Zhao, G. (2022). *In situ* electrochemical spectroscopy for boron-doped diamond electrode reactions: Recent progress and perspectives. *Curr. Opin. Electrochem.* 32, 100892. doi:10.1016/j.coelec.2021.100892

Wei, C., and Chen, C.-H. (2008). The effect of thermal and plastic mismatch on stress distribution in diamond like carbon film under different interlayer/substrate system. *Diam. Relat. Mater.* 17 (7-10), 1534–1540. doi:10.1016/j.diamond.2008.03.004

Wei, J.-j., Zhu, X.-p., Lü, F.-x., and Ni, J.-r. (2011). Comparative study of oxidation ability between boron-doped diamond (BDD) and lead oxide (PbO2) electrodes. *Int. J. Minerals, Metallurgy, Mater.* 18 (5), 589–593. doi:10.1007/s12613-011-0482-1

Wild, C., Herres, N., and Koidl, P. (1990). Texture formation in polycrystalline diamond films. *J. Appl. Phys.* 68 (3), 973–978. doi:10.1063/1.346663

Wild, C., Kohl, R., Herres, N., Müller-Sebert, W., and Koidl, P. (1994). Oriented CVD diamond films: Twin formation, structure and morphology. *Diam. Relat. Mater.* 3 (4-6), 373–381. doi:10.1016/0925-9635(94)90188-0

Williams, O. A. (2011). Nanocrystalline diamond. *Diam. Relat. Mater.* 20 (5-6), 621–640. doi:10.1016/j.diamond.2011.02.015

Witek, M. A., and Swain, G. M. (2001). Aliphatic polyamine oxidation response variability and stability at boron-doped diamond thin-film electrodes as studied by flow-injection analysis. *Anal. Chim. Acta* 440 (2), 119–129. doi:10.1016/s0003-2670(01)01055-8

Wu, H., Xu, F., Liu, Z., Zhou, C., Lu, W., and Zuo, D. (2015). Preparation of large-scale double-side BDD electrodes and their electrochemical performances. *Trans. Nanjing Univ. Aeronautics Astronautics* 32 (6), 674–680.

Xiang-Liu, J., Fang-Qing, Z., Jiang-Qi, L., Bin, Y., and Guang-Hua, C. (1991). "Systematic studies on transition layers of carbides between CVD diamond films and substrates of strong carbide-forming elements," in *SPIE proceedings*. San Diego, CA, United States: Proceedings Volume 1534, Diamond Optics IV. doi:10.1117/12.48293

Xu, S. G. (2016). Modeling and experimental study of electrochemical oxidation of organics on boron-doped diamond anode. *CNL Nucl. Rev.*, 1–15. doi:10.12943/cnr.2016.00018

Yagi, I., Notsu, H., Kondo, T., Tryk, D. A., and Fujishima, A. (1999). Electrochemical selectivity for redox systems at oxygen-terminated diamond electrodes. *J. Electroanal. Chem.* 473 (1-2), 173–178. doi:10.1016/s0022-0728(99)00027-3

Yamaguchi, C., Natsui, K., Iizuka, S., Tateyama, Y., and Einaga, Y. (2019). Electrochemical properties of fluorinated boron-doped diamond electrodes via fluorine-containing plasma treatment. *Phys. Chem. Chem. Phys.* 21 (25), 13788–13794. doi:10.1039/c8cp07402j

Yang, N., Yu, S., Macpherson, J. V., Einaga, Y., Zhao, H., Zhao, G., et al. (2019). Conductive diamond: Synthesis, properties, and electrochemical applications. *Chem. Soc. Rev.* 48 (1), 157–204. doi:10.1039/c7cs00757d

Yang, W., Tan, J., Chen, Y., Li, Z., Liu, F., Long, H., et al. (2022). Relationship between substrate type and BDD electrode structure, performance and antibiotic tetracycline mineralization. *J. Alloys Compd.* 890, 161760. doi:10.1016/j.jallcom.2021.161760

Yano, T., Popa, E., Tryk, D. A., Hashimoto, K., and Fujishima, A. (2019a). Electrochemical behavior of highly conductive boron-doped diamond electrodes for oxygen reduction in acid solution. *J. Electrochem. Soc.* 146 (3), 1081–1087. doi:10.1149/1.1391724

Yano, T., Tryk, D. A., Hashimoto, K., and Fujishima, A. (2019b). Electrochemical behavior of highly conductive boron-doped diamond electrodes for oxygen reduction in alkaline solution. *J. Electrochem. Soc.* 145 (6), 1870–1876. doi:10.1149/1.1838569

Yoon, J.-H., Shim, Y.-B., Lee, B.-S., Choi, S.-Y., and Won, M.-S. (2012). Electrochemical degradation of phenol and 2-chlorophenol using Pt/Ti and boron-doped diamond electrodes. *Bull. Korean Chem. Soc.* 33 (7), 2274–2278. doi:10.5012/bkcs.2012.33.7.2274

Yu, X., Zhou, M., Hu, Y., Groenen Serrano, K., and Yu, F. (2014). Recent updates on electrochemical degradation of bio-refractory organic pollutants using BDD anode: A mini review. *Environ. Sci. Pollut. Res. Int.* 21 (14), 8417–8431. doi:10.1007/s11356-014-2820-0

Yuan, S., Guo, X., Li, P., Mao, Q., Lu, M., Jin, Z., et al. (2021). Insights into the surface oxidation modification mechanism of nano-diamond: An atomistic understanding from ReaxFF simulations. *Appl. Surf. Sci.* 540, 148321. doi:10.1016/j.apsusc.2020.148321

Zanin, H., May, P. W., Fermin, D. J., Plana, D., Vieira, S. M., Milne, W. I., et al. (2014). Porous boron-doped diamond/carbon nanotube electrodes. *ACS Appl. Mater Interfaces* 6 (2), 990–995. doi:10.1021/am4044344

Zhang, C., Lu, X., Lu, Y., Ding, M., and Tang, W. (2019a). Titanium-boron doped diamond composite: A new anode material. *Diam. Relat. Mater.* 98, 107490. doi:10.1016/j.diamond.2019.107490

Zhang, C., Xian, J., Liu, M., and Fu, D. (2018). Formation of brominated oligomers during phenol degradation on boron-doped diamond electrode. *J. Hazard Mater* 344, 123–135. doi:10.1016/j.jhazmat.2017.10.010

Zhang, J., Yu, X., Zhang, Z.-Q., and Zhao, Z.-Y. (2020). Preparation of boron-doped diamond foam film for supercapacitor applications. *Appl. Surf. Sci.* 506, 144645. doi:10.1016/j.apsusc.2019.144645

Zhang, J., Yu, X., Zhao, Z.-y., Zhang, Z., and Li, J. (2019b). Influence of pore size of Ti substrate on structural and capacitive properties of Ti/boron doped diamond electrode. *J. Alloys Compd.* 777, 84–93. doi:10.1016/j.jallcom.2018.10.120

Zhou, M., Liu, L., Jiao, Y., Wang, Q., and Tan, Q. (2011a). Treatment of high-salinity reverse osmosis concentrate by electrochemical oxidation on BDD and DSA electrodes. *Desalination* 277 (1-3), 201–206. doi:10.1016/j.desal.2011.04.030

Zhou, M., Särkkä, H., and Sillanpää, M. (2011b). A comparative experimental study on methyl orange degradation by electrochemical oxidation on BDD and MMO electrodes. *Sep. Purif. Technol.* 78 (3), 290–297. doi:10.1016/j.seppur.2011.02.013

Zhu, C., Jiang, C., Chen, S., Mei, R., Wang, X., Cao, J., et al. (2018). Ultrasound enhanced electrochemical oxidation of Alizarin Red S on boron doped diamond(BDD) anode:Effect of degradation process parameters. *Chemosphere* 209, 685–695. doi:10.1016/j.chemosphere.2018.06.137

Zhu, J. Z., Yang, S. Z., Zhu, P. L., Zhang, X. K., Zhang, G. X., Xu, C. F., et al. (1995a). Electrochemical behaviors of boron-doped diamond film electrodes grown selectively. *Chin. Chem. Lett.* 6 (8), 707–710.

Zhu, P., Zhu, J., Yang, S., Zhang, X., and Zhang, G. (1995b). Electrochemical characterization of boron-doped polycrystalline diamond thin-film electrodes. *Fresenius' J. Anal. Chem.* 353 (2), 171–173. doi:10.1007/bf00322953

Glossary

ACE average current efficiency
AFM atomic force microscopy
AO anodic oxidation
BDD boron-doped diamond
$\mathbf{C_{diamond}}$ purity of chemically vapor deposited diamond
$\mathbf{C_{dl}}$ double-layer capacitance
COD chemical oxygen demand
CTE coefficient of thermal expansion
CVD chemical vapor deposition
EAOP electrochemical advanced oxidation processes
EC energy consumption
EELS electron energy-loss spectroscopy
EF electro-fenton
EIS electrochemical impedance spectroscopy
FWHM full width at half maximum
GDOES pulsed radio frequency glow discharge optical emission spectroscopy
HER hydrogen evolution reaction
HFCVD hot-filament chemical vapor deposition
HPLC high-performance liquid chromatography
HTHP high pressure-high temperature
ICE instantaneous current efficiency
$\mathbf{J_{appl}}$ applied current density
$\mathbf{J_{cut\text{-}off}}$ arbitrary current density cut-off
Jlimit limiting current density
MCD microcrystalline diamond
MCE mineralization current efficiency
MPCVD microwave plasma chemical vapor deposition
NCD nanocrystalline diamond
NDC non-diamond carbon
NDP neutron depth profile
OEP oxygen evolution potential
OER oxygen evolution reaction
PEF photoelectro-Fenton
Q' average charge required for pollutant degradation
$\mathbf{Q^t}$ average charge
RF radio frequency
RFCVD radio frequency plasma chemical vapor deposition
SEF sonoelectro-fenton
SEM scanning electron microscopy
SHE standard hydrogen electrode
SIMS secondary ion mass spectrometry
SLR systematic literature review
SPEF solar photoelectro-fenton
TOC total organic carbon
UNCD ultra-nanocrystalline diamond
UV ultraviolet
XPS x-ray photoelectron spectroscopy
$\boldsymbol{\beta}$ figure-of-merit or the Raman quality fraction
$\boldsymbol{\eta_c}$ combustion efficiency